Metal-Nitrogen-Doped Carbon Single-Atom Electrocatalysts for CO_2 Electroreduction

Liping Huang[a,b], Wenyao Li*[a,c], Min Zeng*[b,e], Guanjie He[c,d], Paul R. Shearing[c], Ivan P. Parkin[d] and Dan J. L. Brett[c]*

[a] *School of Materials Engineering, Shanghai University of Engineering Science, 333 Longteng Road, Shanghai 201620, People's Republic of China*

[b] *Key Laboratory of Thin Film and Microfabrication (Ministry of Education), Department of Micro/Nano Electronics, School of Electronic Information and Electrical Engineering, Shanghai Jiao Tong University, 800 Dong Chuan Road, Shanghai 200240, People's Republic of China*

[c] *Electrochemical Innovation Lab, Department of Chemical Engineering, University College London, London WC1E 7JE, UK.*

[d] *Christopher Ingold Laboratory, Department of Chemistry, University College London, 20 Gordon Street, London WC1H 0AJ, UK*

[e] *State Key Laboratory for Oxo Synthesis and Selective Oxidation, Suzhou Research Institute of Lanzhou Institute of Chemical Physics, Chinese Academy of Sciences, Lanzhou, 730000, People's Republic of China*

Corresponding authors: wenyao.li@ucl.ac.uk (Wenyao Li); minzeng@sjtu.edu.cn (Min Zeng); d.brett@ucl.ac.uk (Dan J. L. Brett)

Abstract: The application of the electrocatalytic CO_2 reduction reaction (CO_2RR) to high-value-added carbon items is an incredibly encouraging course for the mitigation of greenhouse gas emissions. However, the effective design of CO_2RR electrocatalysts with high proficiency, great selectivity, and robust stability presents serious challenges. Electrocatalytic CO_2RR involves complicated mechanisms due to multiple electron/proton transfer processes, resulting in various intermediates. To further understand the mechanism of CO_2RR, single atomic site catalysts represent a simplified catalytic model which can also lead to improvements in catalytic activity. On account of the unique electronic and geometric structures, metal-nitrogen-doped carbon (M-N-C) single-atom electrocatalysts have energizing possibilities for the CO_2RR, and are a potential substitute for noble metal catalysts. This review pays attention to the recent advancements of M-N-C catalysts for the CO_2RR, which include the synthesis, characterization, and performance. Combining experimental and theoretical aspects, it is found that new insight is being achieved into the role of active sites on the reaction mechanism. Finally, approaches to the design of electrocatalysts for CO_2RR and future research directions are discussed.

Keywords: CO_2 reduction reaction (CO_2RR); Electrocatalytic reduction; Single atomic site catalysts; Metal-nitrogen-doped carbon (M-N-C); Mechanism

Table of Content

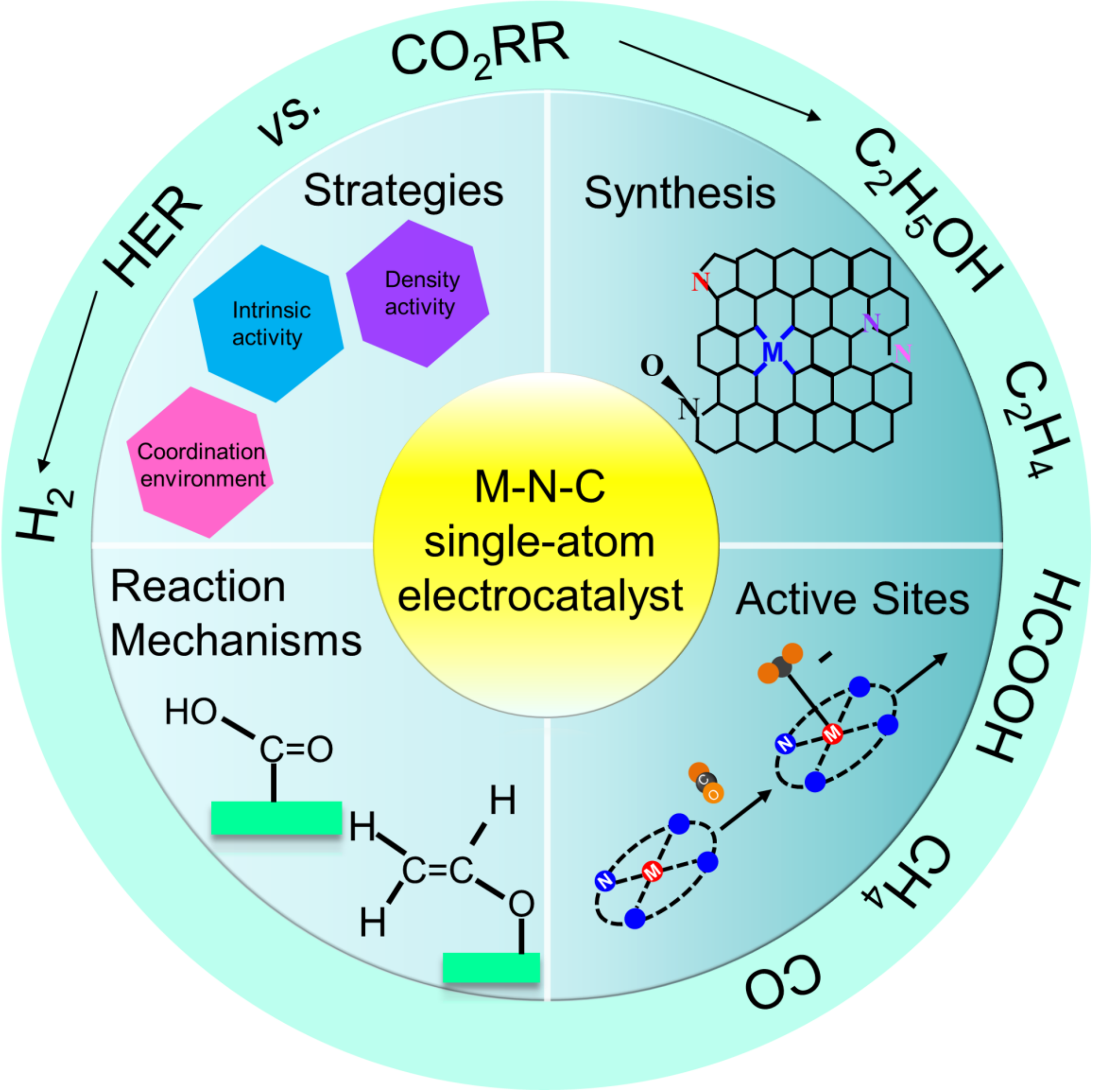

1. Introduction

The increasing concentration of atmospheric CO_2 and its effect on global warming and ocean acidification is arguably the greatest challenge facing humanity [1]. Yet with rapidly growing economies and global populations, we continue to rely on ever-depleting fossil fuels for power generation and transportation [2-5]. The efficient conversion of CO_2 into carbon-based chemicals and fuels is, therefore, a compelling need [6, 7]. For CO_2, the high bond energy of C=O (750 kJ mol^{-1}) means that activating the CO_2 molecule requires a high overpotential. The process of CO_2 electroreduction is also kinetically sluggish on account of it being a multi-proton process coupled with electron transfer [8]. So efficient electrocatalysts are necessary for improving the performance of electrocatalytic CO_2RR. In the process of electrochemical catalytic reduction, the catalytic hydrogenation reaction of CO_2 occurs directly on the cathode surface. The mechanism of electrochemical catalytic reduction of CO_2 is very complex. The electrochemical reduction of CO_2 on different electrocatalyst surfaces can be accomplished by losing 2, 4, 6 and 8 electrons of CO_2. The final products of CO_2RR variably involve CO, HCOOH, CH_3OH, C_2H_5OH, HCHO, CH_4 and C_2H_4, *etc*. The related half-reactions and thermodynamic equilibrium potentials are shown in Fig. 1. In general, CO_2 electrochemical catalytic reduction products are not single species, but mixtures. Its selectivity and faraday efficiency depend on many factors, such as the type of electrode material, the properties of catalyst, electrolyte solution, and applied voltage [9].

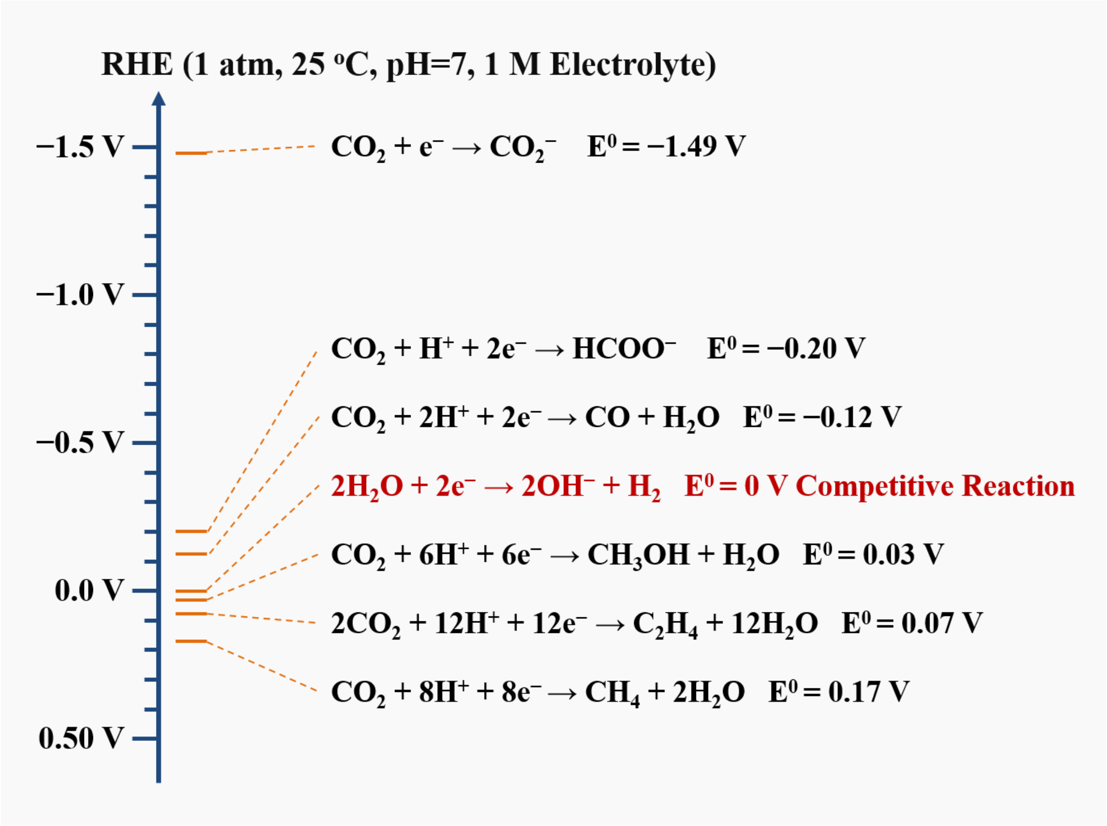

Fig. 1 Thermodynamic equilibrium potential (versus reversible hydrogen electrode (RHE)) diagram of various products produced by electrocatalytic CO_2RR in the aqueous electrolyte (pH=7).

The theoretical redox potentials of various CO_2RR products are tightly clustered, resulting in competing processes which include the hydrogen evolution reaction (HER) [10, 11]. Besides, the various catalytic pathways at higher overpotentials always result in different products which affect the selectivity [12]. Many studies have demonstrated that catalysts can be designed to be conducive for the activation of CO_2, especially after tuning the geometry and electronic structure [13, 14]. The efficient CO_2RR electrocatalysts can combine with the reaction intermediate at an appropriate strength with significant inhibition for the competitive HER [15, 16].

The product type of CO_2RR is greatly influenced by the cathode electrode materials. In the past few decades, a range of electrocatalysts have been developed for CO_2RR

[17], such as noble metals [18, 19], transition metals [20-23], molecular metal complexes [24-26], metal-organic frame materials [27-29], carbon-based materials [30, 31] and N mixed carbon-based materials [32, 33]. Most of these studies focus on noble metal-based catalysts [34, 35]. For instance, silver and gold are demonstrated to selectively reduce CO_2 to CO at low overpotentials [15, 36]. However, considering their high price and low abundance, they are not conducive to large-scale production.

In recent studies, transition metal-doped nitrogenated carbon materials, which are commonly described as M-N-Cs (M = Ni, Co, Zn, Fe, W, Mn, Cu, Mo, *etc.*), have been considered as promising candidates for precious metal catalysts [37]. M-N-Cs are a rapidly developing type of single-atom catalyst (SAC) [38, 39], and deliver the following advantages: (i) they maximize the efficiency of metal-atom utilization, nearly 100%; (ii) metal atoms are highly dispersed and result in high exposure of active sites; (iii) they have a relatively uniform active center; (iv) the central metal ions with low coordination number provide an ideal model system to study the catalytic mechanism [40-43]. Furthermore, based on the carbon substrate, M-N-Cs also have additional advantages such as good chemical stability, outstanding electrical conductivity, enormous specific surface area, controllable porous structure, and feasible preparation with low cost [31, 44, 45]. M-N-Cs share a unique network structure with numerous marginal sites and abundant active sites, which is beneficial to electron transport [46, 47]. Profiting from those characteristics, there has been significant improvement in M-N-Cs for electrocatalytic CO_2 reduction in recent years [48-50].

Several excellent reviews have been published to summarize the effectiveness of metal nitrogen-doped carbon (M-N-Cs) electrocatalysts, for instance, Lee's research group reviewed the recent research progress, including photocatalysis, electrocatalysis, supercapacitors, rechargeable batteries, etc. based on two-dimensional transition metal sulfides (TMD), transition metal nitride (TMN), transition metal sulfides (TMS) and MXenes nanomaterials [11, 14, 21-23], which not only promote the research in this field to a new stage, but also provide inspiration for many other electrocatalytic reactions involving gases, while nearly none have reviewed from the perspective of the specific factors that affect the intrinsic catalytic activity and clarify the reasons from the mechanism. Herein, we aim to systematically summarize the recent achievements on metal-nitrogen-doped carbons (M-N-Cs) which are active and robust electrocatalysts for the CO_2RR. Furthermore, combining experimental with theoretical studies, new insights into the role of active catalytic sites and reaction mechanisms are discussed. Finally, perspectives on the design of CO_2RR electrocatalysts are summarized and new research directions are identified.

2. Metal-nitrogen-doped carbons

2.1 Preparation methods

The discovery of single-atom catalysts (SACs) dates from 1995, Thomas and colleagues applied the epoxidation of cyclic to develop a Ti single-site heterogeneous catalyst [51]. In 2011, Zhang and co-workers applied single Pt atoms for CO oxidation through the co-precipitation technique and the conception of single-atom catalysts firstly comes into people's field of vision and research [52]. So far, a series of preparation methods have been created to synthesize SACs, for instance, mass-selected soft-landing [53-55] and atomic layer deposition (ALD) methods [56, 57] have been proved to be powerful for precise control of the formation of SACs (Fig. 2a). Wet-chemistry approaches, including co-precipitation [58, 59] and impregnation method [60, 61], are at present viewed as the most basic and effective strategies (Fig. 2b). High-temperature pyrolysis is an effective approach through the heat treating selected precursors at optimal pyrolysis temperatures [62]. Traditional, the precursors always contain metal salts, carbon sources, and coordination or doped nonmetal atoms (e.g., N, P, S). These precursors are usually pyrolysis under different gas, such as N_2, Ar, H_2, NH_3 and sometimes mixtures of them. As the typical branch of SACs, the M-N-C structure originates from macromolecular heterocyclic compounds such as porphyrins and phthalocyanines [63, 64], and has been studied extensively as an electrocatalyst to convert CO_2 to CO.

In general, the M-N-C catalysts are usually synthesized through the annealing of a mixture containing inorganic metal salts, nitrogen precursors, and carbon reactants (*i.e.*, graphene, carbon nanotubes (CNTs), and porous carbon) at high temperature in inert environments [65]. During the annealing process, inorganic metal salts convert to metal nanoparticles, and nitrogen atoms are doped into the carbon structure to form different chemical functionalities, including pyridinic, graphitic and pyrrolic, generating active $M\text{-}N_x$ single sites and nitrogen-doped carbon sites (N-C) (Fig. 2c). These special structures enhance the content of active sites and improve the charge transfers process, facilitating the electrocatalytic performance with synergistic effects [47, 66]. In recent years, Metal-Organic Framework materials (MOFs) have been used to be viable precursors/templates to prepare single-atom catalysts materials via pyrolysis due to their adjustable molecular structure and chemical and topological diversity. For instance, by pyrolyzing ZIF-8 under an argon atmosphere in the presence of copper foam (Fig. 2d), Qu et al. obtained the controllable Cu-SAs/N-C [67]. Deng et al. achieved the controllable preparation of Co single-atoms (SAs) on carbon support using ZIF-67 precursors [68]. In summary, the high-temperature pyrolysis method has broad industrial application prospects in the synthesis of M-N-Cs which can decrease the cost of noble metal and present a feasible method to prepare high-performance electrocatalysts for a large scale.

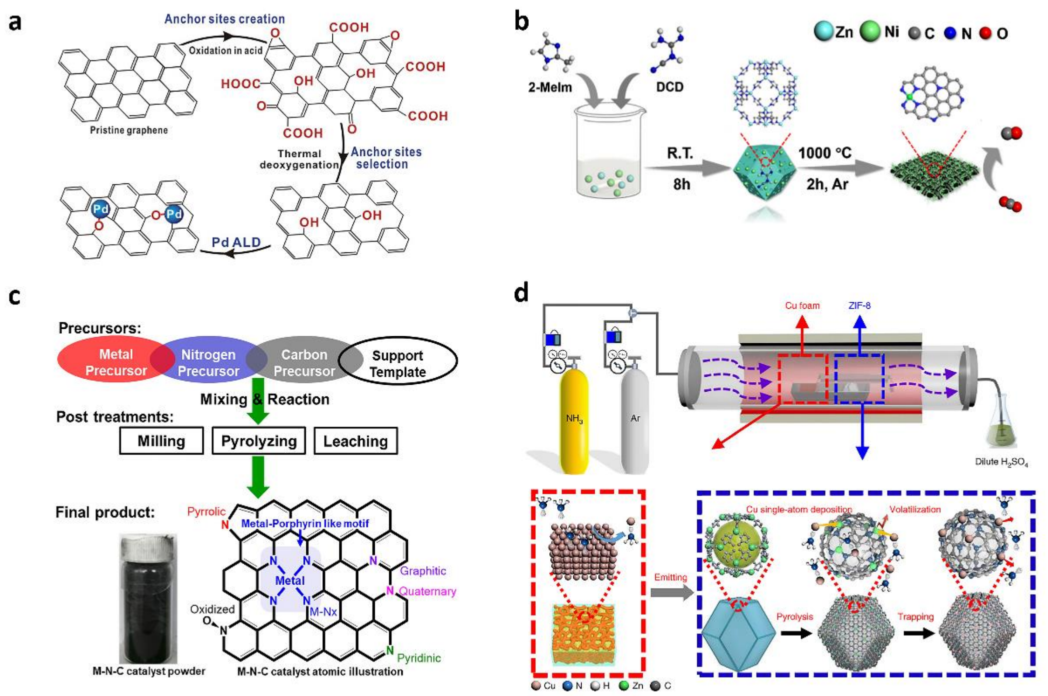

Fig. 2 (a) Single-atom Pd catalyst synthesis via ALD methods. Reproduced with permission [57], Copyright © 2015, American Chemical Society. (b) Synthesis of Ni SAs/NCNTs via co-precipitation methods. Reproduced with permission [69], Copyright 2018, Elsevier. (c) Common preparation for M-N-Cs. Reproduced with permission [65], Copyright © 2019, American Chemical Society. (d) Schematic of the preparation of MOF-derived single-atom catalysts. Reproduced with permission [67], Copyright © 2018, Springer Nature.

2.2 Characterization methods

As mentioned earlier, the possibility of single-atom catalysts has been discovered in 1995 before it was clearly presented, nevertheless, the limited characterization techniques at that time restricted the comprehensive judgment on the atomic scale and hindered the evolution of single-atom catalysts. With the development of advanced characterization techniques, many characterization methods have been used to observe the reaction intermediates, recognize the active centers, and survey the dynamic catalytic performance. Except for that conventional SEM, TEM, XRD, and XPS can characterize the morphology of catalyst materials and the chemical change quantitatively, scanning transmission electron microscopy (STEM) and scanning tunneling microscopy (STM) can directly obtain the surface morphology characteristic image of single metal atoms [67, 70]; X-ray absorption spectroscopy (XAS) and extended X-ray absorption fine structure (EXAFS) [71] spectroscopy can obtain structural information such as atomic spacing and coordination number (Fig. 3).

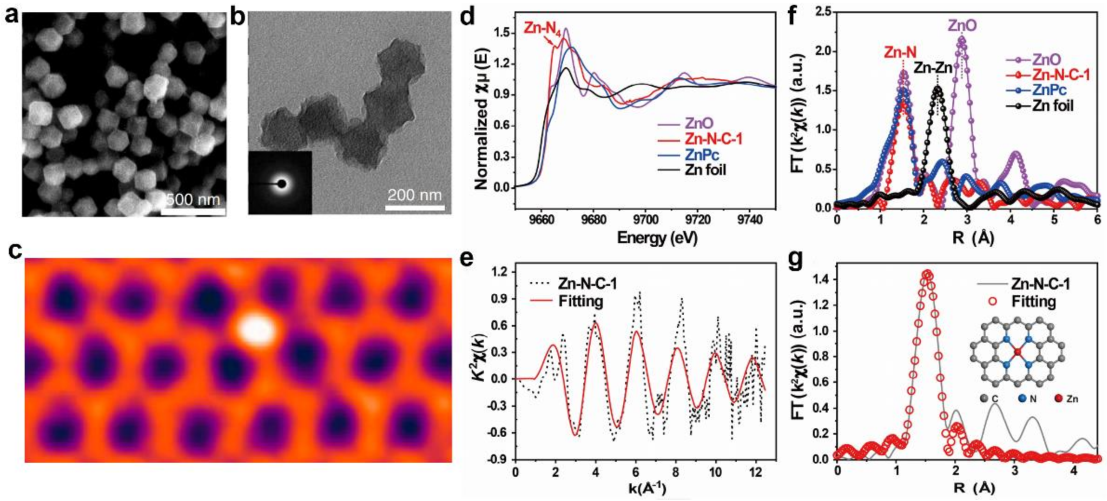

Fig. 3 (a-b) SEM and TEM images of ZIF-8. Reproduced with permission [67], Copyright © 2018, Springer Nature. (c) AC-TEM images of Fe single atoms. Reproduced with permission [70], Copyright © 2014, American Chemical Society. (d-g) XAS measurements of the Zn single atom. Reproduced with permission [71], Copyright © 2019, John Wiley and Sons.

2.3 Influence factors for catalyst performance

In studying the CO_2RR, Hori [72] reported the analysis of products on various metal electrodes. Generally, the catalysts can be ranked into four product categories: HER metals [73], CO producing metals [74, 75], formic acid-producing metals [76], and various other products reduced on Cu which are capable of converting CO_2 to hydrocarbons via the $2e^-$ reduction pathway [77, 78].

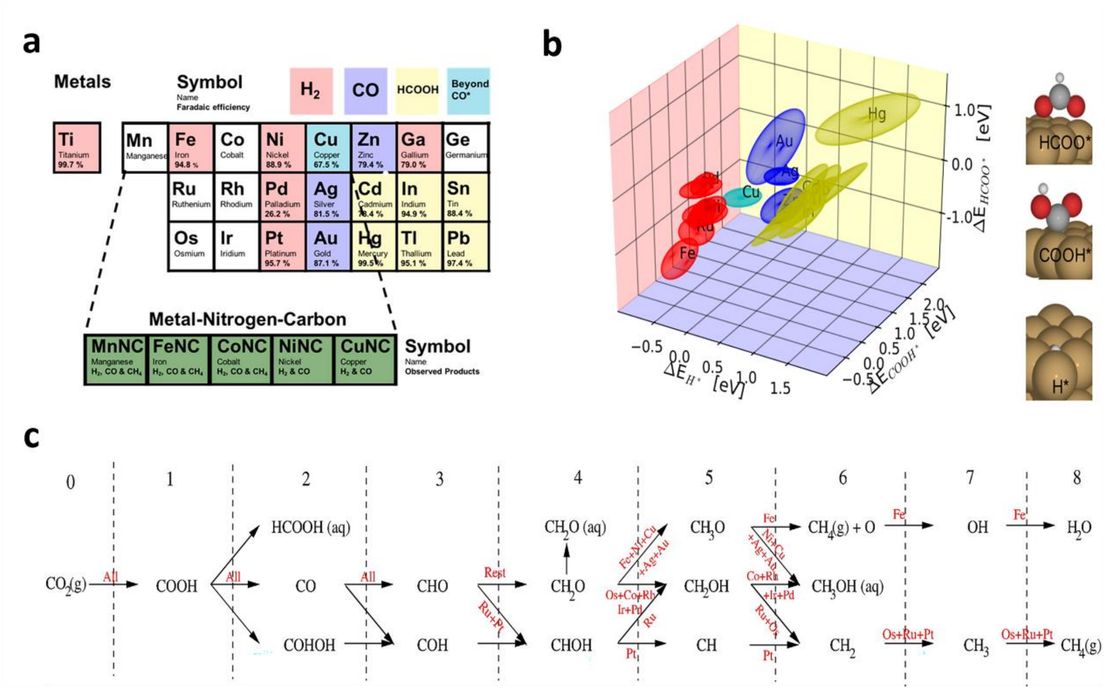

Fig. 4 (a) Classification of metal catalysts for CO_2RR from experiments by Hori. Reproduced with permission [65], Copyright © 2019, American Chemical Society. (b) Combined plot of the three-dimensional space of descriptors in CO_2 electroreduction towards different products. Reproduced with permission [12], Copyright © 2017, John Wiley and Sons. (c) Reaction paths of electrochemical CO_2 reduction on a range of transition metals. Reproduced with permission [79], Copyright © 2013, American Chemical Society.

In Fig. 4a, a partial periodic table is displayed grouped according to four product types. The single-atom transition metal M-N-C catalysts commonly discussed are displayed in the corresponding box written with the products. Alexander Bagger et al. [12] constructed a three-dimensional binding energy plot to classify the three products by the three intermediates (Fig. 4b). In 2013, Tripkovic et al. [79] built up a hypothesis to declare porphyrin-like metal hybridized with graphene, from which they claimed that these materials could be active for CO_2RR and the intermediate product CO can be further converted to CH_4 or MeOH, depending on the metal center (Fig. 4c) [80, 81]. Since then, several M-N-C electrocatalysts with different metal centers have been widely discussed as a promising alternative for CO_2RR [69, 82-86]. For instance, Pan et al. [87] reported an investigation of the effects of five metal centers (M= Ni, Co, Fe, Mn, Cr) on CO_2RR performance and mechanisms. Menisa et al. [88] prepare a family of M-N-C (M= Ni, Co, Fe, and Cu) through facile pyrolysis to prove that selective reduction of CO_2 strongly depends on the nature of the metal center. They suggested that Ni and Fe have higher energy in M-N-C than Co, Mn, Cr and Cu for the electrocatalytic CO_2RR to CO. The role of Fe atom-based active site is to reduce overpotentials and Ni atom-based active site can effectively enhance CO selectivity and reaction rates [89, 90].

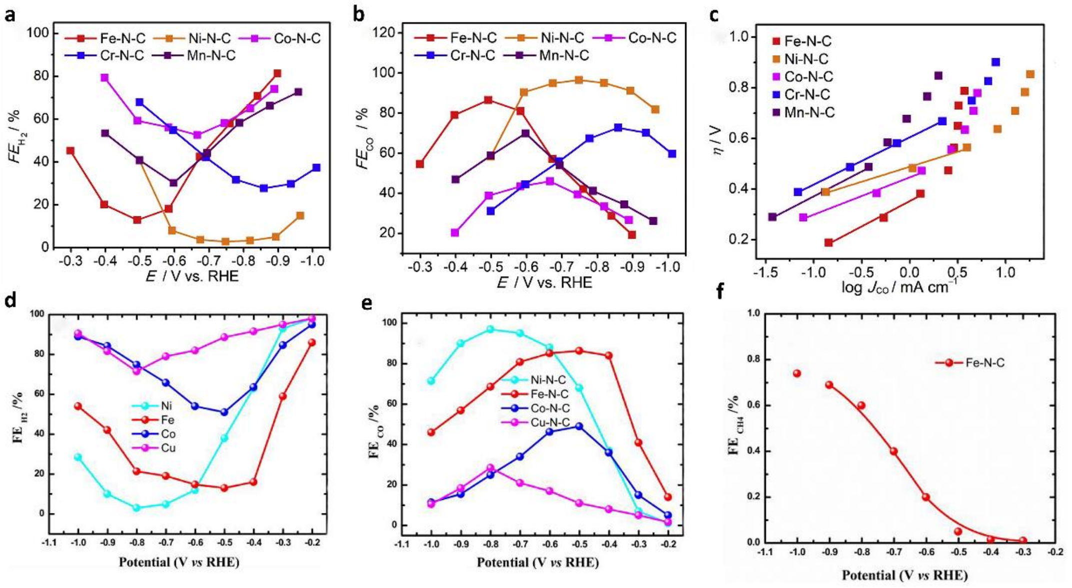

Fig. 5 (a) Faraday efficiency (FE) of H_2 and (b) CO for M-N-C. (c) Tafel plots of current densities of CO reduction *vs*. overpotentials for different M-N-C. Reproduced with permission from Reference [87], Copyright © 2018, Elsevier. (d-f) FEs of H_2, CO, and CH_4 for M-N-C. Reproduced with permission from Reference [88], Copyright © 2020, Royal Society of Chemistry.

The Faradaic efficiency curves (Fig. 5a, b, d and e) indicate that the production of H_2 and CO is potentially dependent, and there is internal competition between CO_2RR and HER. The M-N-C, Fe(or Ni)-N based materials are capable of improving the selectivity for CO, while Co (or Cu)-N-C tends to promote HER [91]. In addition, Fe-N-C exhibited the highest CO reduction performance near more positive potential regions (> − 0.5 V) and can reduce CO_2 to trace of CH_4 (Fig. 5f), whereas Ni-N-C shows the best CO reduction activity at potentials <− 0.75 V. The Tafel slope of Ni-N-C is the lowest, followed by Co-N-C, Cr-N-C, Mn-N-C and Fe-N-C (Fig. 5c). Overall, it was found that Fe, Co and Ni possessed lower overpotential and excellent selectivity toward H_2/CO/CH_4. This implies that it is possible to selectively dope these metal centers into various nanocarbon architectures to design high-performance M-N-C for CO_2RR, especially for high-value chemical fuel production [92, 93]. Cu and Cu-based materials are the only existing heterogeneous catalysts capable of electrochemically reducing CO_2 via a $2e^-$ pathway to produce CH_4. Zhao et al. [94] reported the array of copper sulfide nanosheets loaded on nickel foam (CuS@NF) as an efficient electrocatalyst for the reduction of CO_2 to CH_4. Moreover, CuS nanosheets possess high faradaic efficiency and stable capability due to the nanosheet structure and the attendance of S species. More recently, monoatomic Zn has attracted extensive attention because it can also electrocatalytically reduce CO_2 to hydrocarbons under certain conditions. Han et al. [95] anchored structured Zn single atoms (SAs) onto microporous N-doped carbon (SA-Zn/MNC), which has excellent catalytic performance and stability for electrocatalytic reduction of CO_2 to CH_4. This stable and excellent performance can owe to the rapid charge transport resulting from the conductivity of the carbon matrix, micropores for active site exposure. For the sake of proving their predictions and further realize activity/selectivity order, Hu et al. [85] studied a class of transition metal (*i.e.*, Ni, Co and Fe) nitrogen-doped porous carbon (M-N-C) catalysts for CO_2RR. The results indicated that doping with different metals can significantly improve its activity. The activity follows the order Ni, Fe ≫ Co, while the selectivity sequence is Ni > Fe ≫ Co in an aqueous solution.

Furthermore, the electrocatalytic CO_2RR performance of M-N-Cs not only depends on the types of metal centers, but also relies on the structure and proportion of material and reaction conditions (e.g., temperature and pH) [96-103]. Huan et al. [97] obtained a series of Fe-N-C catalysts with adjustable ratios of single-Fe atoms and Fe nanoparticles, and they deeply investigated the effects of structural parameters on the performance of CO_2RR (Fig. 6). The result indicated that FeN_4 moieties are the essential active centers for the selective reduction of CO_2 to CO, while Fe nanoparticles play a role in catalyzing the hydrogen evolution reaction. Besides, increasing Fe loading leads to an increase in the amount of Fe nanoparticles (Fig. 6a).

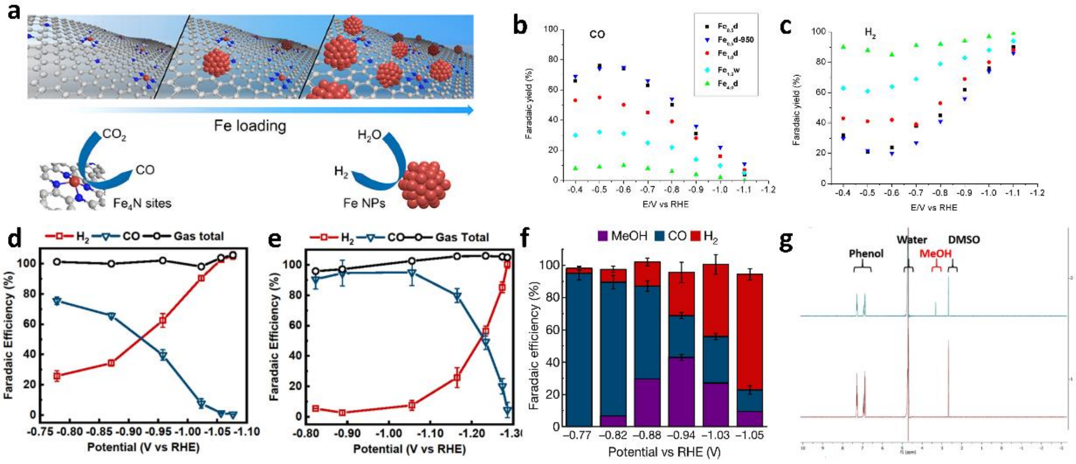

Fig. 6 (a) Schematic diagram of the Fe-N-C materials. Red stands for Fe atoms, grey for C atoms, and blue for N atoms. (b) Faradaic yield for CO and (c) H_2. Reproduced with permission from Reference [97], Copyright © 2017, American Chemical Society. (d-f) Potential-dependent performance for electrocatalytic CO_2 reduction through FePc/CNT, NiPc/CNT and CoPc/CNT. (g) 1H NMR spectra after CO_2 electroreduction electrolysis. Reproduced with permission from Reference [104], Copyright © 2019, Springer Nature.

Fig. 6 b-c reveal the highest selectivity of CO reduction is obtained with a low weight of Fe in the precursors ($Fe_{0.5}$d and $Fe_{0.5}$d-950), while the catalysts containing a large relative fraction of crystalline Fe ($Fe_{1.0}$w and $Fe_{4.0}$d) display a high Faradaic yield for H_2 at all potentials (Fig. 6c), especially in the more negative potential range. Thus, the proportion of FeN_4 moieties in Fe nanoparticles selectively controls the formation of CO rather than promotes HER. Therefore CO/H_2 ratios can be controlled by adjusting the percentage of FeN_4 to meet the requirement of various chemical liquid fuels. Similarly, Leonard et al. [98] prepared various porous iron-nitrogen-carbon (Fe-N-C) electrocatalysts from different nitrogen precursors. These catalysts possessed distinctly different physical properties, such as different proportions of chemical N-functionalities or absorption surface areas, which can observably improve the performance of CO_2 reduction reaction in aqueous media.

To further understand how the content of each component in the catalyst affects the catalytic performance, Wang and co-workers [105] synthesized a series of Pd@Au electrocatalysts by modifying Au nanoparticles with controlled amounts of Pd, The results indicated that the catalytic activity of CO_2 reduction to CO showed a nonlinear correlation with the content of Pd, which is attributed to the change of adsorption energy of *CO and *COOH at various Pd sites. Zhang's group [106] prepared a series of defective N-doped carbon spheres (D-NC-X, where X represents the heat treatment temperature) for electrocatalytic carbon dioxide reduction reaction. The experimental results showed that the CO_2RR performance of these catalysts was positively correlated with defect concentration, while negatively correlated with nitrogen content. DFT calculations showed that the introduction of intrinsic carbon defects changed the local charge density of carbon atoms, making it easier to activate CO_2 molecules to form the active intermediate COOH*, and then to form CO.

Furthermore, in addition to the properties of metal precursors, the microstructure of the carbon has a crucial influence on the adsorption of CO_2 to the active centers which affect the overall electrocatalytic performance [31]. Because the strong metal-carrier interaction between the well-dispersed metal monatomic and the carbon substrate can not only inhibit the aggregation of metal atoms, but also adjust the geometric structure and electron configuration of the active catalytic sites. Graphene exhibits an excellent electrical conductivity in favor of electron transport and a considerable specific surface area allows for exposing high-loaded active centers, which are beneficial to improve the catalyst performance of single-atom catalysts [107-109]. Furthermore, the electronic coupling between the modified metal catalyst and the graphene substrate can be easily regulated, as well as the electronic states of modified metal active centers [70, 74]. Thus the output performance of graphene-supported electrocatalysts can be controlled correspondingly. For instance, Wang et al. [110] prepared a multiphase molecular Co electrocatalyst by immobilizing planar Co(II)-2, 3-naphthalocyanine (NapCo) complex on doped graphene under mild conditions. The catalyst has excellent catalytic activity and can selectively reduce CO_2 to CO with high faradic efficiency in an aqueous solution.

Carbon nanotubes have adjustable nanotube cavity structures, suitable pore size distribution to facilitate better dispersion of metal components, and a larger specific surface area to fill and absorb particles. And it can be modified in different ways according to people's need to make it suitable as a new catalyst carrier [8]. For instance, Wu et al. [104] studied metal phthalocyanine (M=Fe, Co and Ni) molecules decorated on carbon nanotubes (CNTs) as electrocatalysts to explore that CO_2 can be further reduced to MeOH in M-N_4-based species. The result indicates MPc/CNT (M=Fe, Ni or Co) electrocatalysts demonstrate a great selectivity of CO reduction in the medium overpotential region. The faradaic efficiency (FE) of CoPc /CNT and NiPc /CNT for CO was up to 95%, while the selectivity of FePc /CNT for CO was about 80%. At more negative electrode potentials, NiPc/CNT and FePc/CNT only produce H_2 (Fig. 6d-f). Interestingly, CoPc/CNT can generate methanol (MeOH), which is further confirmed by both 1H and 13C nuclear magnetic resonance (NMR) spectroscopy (Fig. 6g). CoPc/CNT catalyzes the electroreduction of CO_2 to MeOH, which is caused by the synergistic effect of the following factors. Firstly, CoPc is dispersed on highly conductive CNTs as a single molecule, which is conducive to transfer continuous electrons on the active centers to achieve the multi-electron reduction of CO_2. Secondly, the type of carbon carrier is important because CoPc molecules are fixed to the carrier and receive electrons from the carrier. Thirdly, CoPc is inactivated under reduction conditions. All of these examples demonstrate the importance of the active sites and the structure of catalysts for CO_2RR.

The temperature of the heat treatment can affect the structures of the materials, and further influences the activity of catalysts towards the CO_2 reduction reaction [96, 110]. González-Cervantes and co-workers [96] prepared five Fe-N-C catalysts under different pyrolysis temperatures. The result shows that the catalyst annealed at the lowest temperature displays the highest activity while the selectivity is enhanced with increasing synthesis temperature. That is because the annealing temperature influences both the ratio between the different N functionalities and the electrochemical surface area. As shown in Fig. 7a and 7b, it is confirmed that higher annealing temperature is beneficial to improve the selectivity towards the CO_2RR for the catalysts. On the whole, the FE_{co} increases with the rise of temperature under a certain range of potential, whereas different pyrolysis temperatures lead to different degrees of influence on the selectivity of FE_{CH4}. Likewise, Chen et al. [111] prepared Zn-N-G electrocatalysts through continuous high-temperature annealing and acid etching, aiming to study the effect of annealing temperature on electrocatalytic performance. The total current density (j_{total}) raises with the potential for Zn-N-G electrocatalysts prepared at different pyrolysis temperatures (Fig. 7c). Besides, Zn-N-G-800 shows the highest selectivity for CO among these catalysts (Fig. 7d). In brief, the selectivity towards the single product of CO_2RR can be regulated by controlling the pyrolysis temperature and different active metal centers have different optimum temperatures toward CO_2RR.

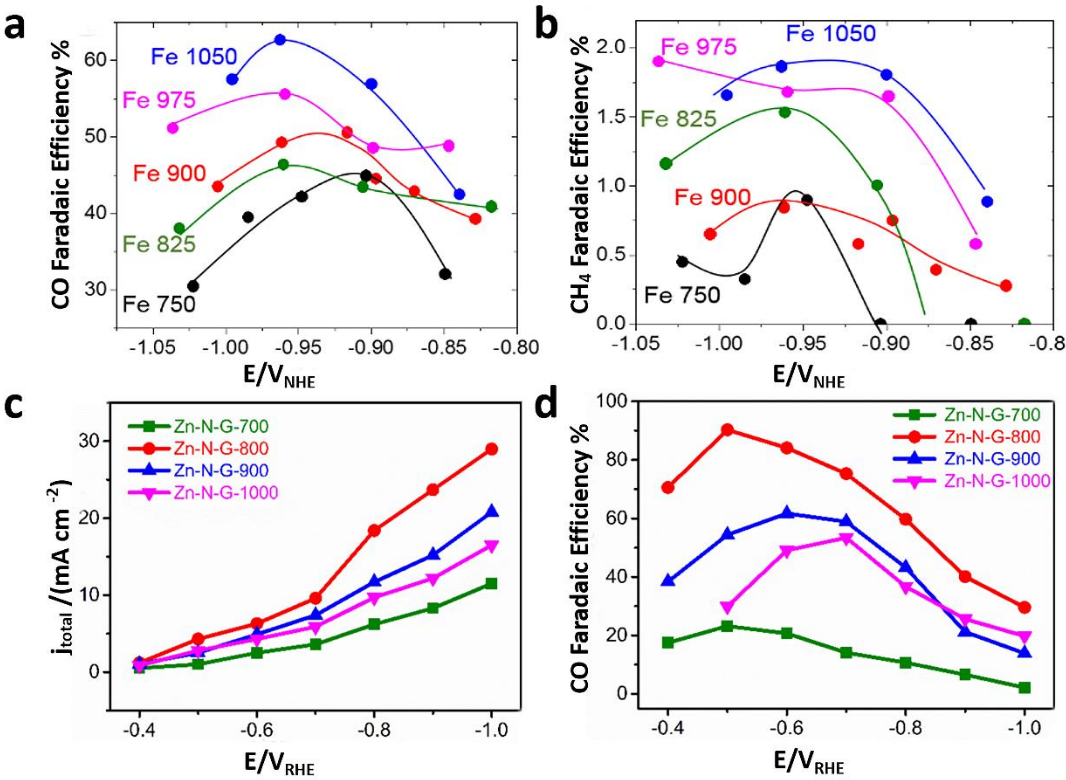

Fig. 7 (a) CO Faradaic efficiency. (b) CH_4 Faradaic efficiency in electrolyte KH_2PO_4/K_2HPO_4 (0.1 M) of Fe-N-C. Reproduced with permission from Reference [96], Copyright © 1969, John Wiley and Sons. (c) Total current density. (d) CO Faradaic efficiency. Reproduced with permission from Reference [111], Copyright © 2018, John Wiley and Sons.

Beyond that, the pH and local pH also impact the Faradaic efficiency and the selectivity of the products [112, 113]. Varela [102] performed CO_2 electrolysis in the electrolyte with different pH values to explore the impact of the pH on the selectivity of CO_2RR and clarify the role of proton concentration. The results indicated that the formation of H_2 and CH_4 is related to the pH of the normal hydrogen electrode (NHE) scale, while the generation of CO has no direct relevance to pH, indicating that is the rate-limiting step for CO reduction is decoupled proton-electron transfer (DPET). Furthermore, different pH values influence the selective formation of CO or H_2 in the CO_2RR process which provides a chance to regulate the CO/H_2 ratio.

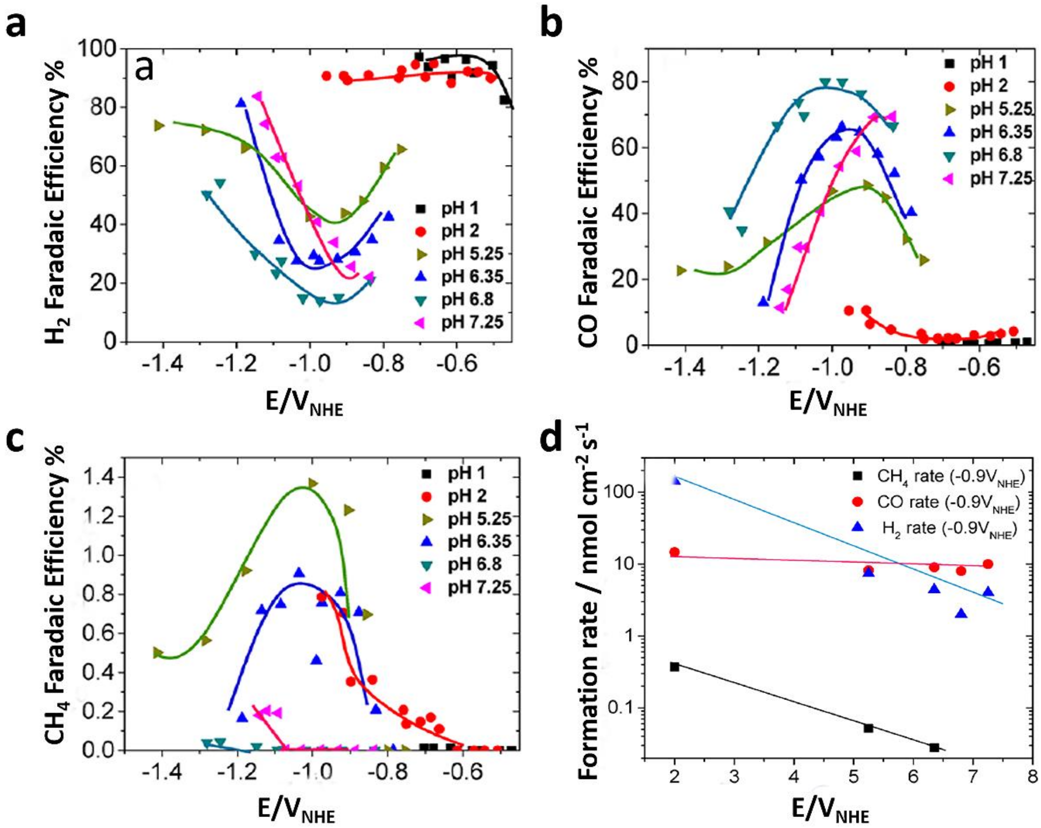

Fig. 8 (a-c) Faradaic efficiency of H_2, CO and CH_4 at different pH. (d) Product formation rates of CH_4, CO and H_2. Reproduced with permission from Reference [102], Copyright © 2018, American Chemical Society.

Fig. 8 a-c shows the FE of H_2, CO and CH_4, respectively. It is clear that HER prefers an acidic environment. In contrast, CO prefers neutral, while alkaline conditions and near-neutral pH in favor of methane synthesis. However, H_2 is the main product and only a little CO or methane is formed in the acidic condition. Over the pH range of the research, the Faradaic efficiency for methane generation is highest at pH=5.25. Furthermore, the formation rate of CO doesn't change with potential (Fig. 8d), which reflects that the rate-potential relationship of CO tends to a straight line at all pH values. Whereas, different from CO production, the formation of CH_4 and H_2 shows obvious Nernstian pH dependence. Therefore, the bulk electrolyte affects the selectivity for CO_2RR. In conclusion, the production of H_2 is strongly dependent on pH, while the production of CO is independent. Thus, the ratio of CO/H_2 during the electro-reduction of CO_2 can be easily adjusted by controlling the pH of the reaction solutions to meet the requirement of high selectivity toward CO, meanwhile suppressing the HER.

The mass loading (i.e. the density of active sites) is the key factor affecting the final catalytic performance. The performance is best only when the mass loading reaches the surface monodisperse. Once the mass loading exceeds this threshold, agglomeration and sintering phenomenon will occur, which is not conducive to the dispersion of the catalyst and the performance. Qin et al. [114] prepared Co/TiO_2 catalysts with different Co mass loading by a sedimentation-deposition method to catalyze CO_2 methanation reaction. The result shows that with the increase of Co mass loading, the average size of Co particle first increased and then reduced. In the meantime the average pore diameter increased, leading to the decrease of the pore volume and specific surface for catalysts. More importantly, smaller Co particles were more conducive to the CO_2 methanation reaction.

In conclusion, the electrocatalytic CO_2RR performance of M-N-Cs is affected by multiple factors. The active metal center in materials takes an extremely important effect during the process of CO_2RR. For example, Fe has been demonstrated to selectively catalyze CO formation at low overpotentials and can convert CO to CH_4. Whereas Ni-based materials are highly selective for CO production and can easily facilitate the reaction rate. However, the catalyst structure, composition, and reaction conditions are also dominant factors for catalytic performance. For example, acidic pH is favorable for the competitive HER process and decreases the selectivity of CO_2RR to other products. Thus, working at neutral or alkaline pH is beneficial to obtain a high selectivity. The mass loading is also crucially important to the performance of catalysts. Therefore, in order to synthesize ideal CO_2RR catalysts with low overpotential, high selectivity, and stability, we should not only pay attention to the optimum metal center, but also select suitable carbon support structures with a large surface area and appropriate reaction conditions. Table 1 summarizes the performance comparison of the above-mentioned M-N-Cs.

Table 1 A summary table of the CO_2RR performance of the above-mentioned M-N-C electrocatalysts

Catalysts	**Electrolyte**	**Product**	**Potential (V *vs.* RHE)**	**FE (%)**	**J (mA cm^{-2})**	**Stability**	**TOF (h^{-1})**	**Ref.**
Ni-N-Gr	0.1 $KHCO_3$ pH=6.8	CO	-0.7~-0.9	>90	-	5 h	2500	74
NGM/CP	ILs ([Bmim]BF_4)	CH_4	1.4	93.5	1.42	5 h	-	114
NG-800	0.1 $KHCO_3$ pH=6.8	CO	−0.58	85	~1.8	-	-	115
CN-H-CNT	0.1 $KHCO_3$	CO	-0.5	88	-	24000 s	-	33
Sn	0.1 $KHCO_3$ pH=6.8	$HCOO^-$	-0.8	70	~8-10			76
Fe-N-C	0.5 $KHCO_3$	CO	-0.5	80	7.5	-	-	97
Cu_2O-derived Cu	0.1 $KHCO_3$ pH=6.8	C_2H_4 CH_4	-0.98 -1.13	32.4 <2	-	-	-	116
NDC-700	0.5 $KHCO_3$	CO	-0.82	83.7	-8	72 h		117
Ni−N_4-C	0.1 $KHCO_3$	CO	-0.81	99	28.6	-	-	118
Ni SAs/N-C	0.5 $KHCO_3$	CO	0.89	>71.9	7.37	-	5273	84
CuS@NF	0.1 $KHCO_3$	CH_4	-1.1	73 ± 5%	-	60 h	-	119
Ni^{2+}@NG	0.5 $KHCO_3$	CO	-0.68	92	10.2	-	-	120
Zn-N-G-800	0.5 $KHCO_3$	CO	0.39	91	11.2	15	-	111
FeNC	0.1 $KHCO_3$	CO	-0.6	85	>5	-	-	98
Ni−N-C	0.1 M $KHCO_3$	CO	0.65	96	-8.2	550 min	1060	87
NFe-CNT/CNS	0.1 $KHCO_3$ pH=6.8	CO	0.48	69	0.82	-	-	122
Co−N_5/HNPCSs	0.2 M $NaHCO_3$	CO	-0.73	99.2	6.2	10 h	-	123
C-ZnxNiy ZIF-8	1 M $KHCO_3$	CO	-1.03	92~98	71.5 ± 2.9	-	10087±216	44

ZnNx/C	0.5 $KHCO_3$	CO	-0.43	95	-4.8	>75 h	9969	124
Fe–N–G/bC	0.1 $KHCO_3$ pH=6.8	CO	0.55	~95	-	12 h	-	125
Fe−N−PC	0.5 $KHCO_3$	CO	-0.49	~90	11.44	-	-	90
Ni-N-MEGO	0.5 $KHCO_3$	CO	-0.55	~89	~19.3	21 h	0.24 s^{-1}	126
MNC-D	1 M $KHCO_3$	CO	-0.58	~92	-6.8	16 h	-	127
Zr-DMBD	CH_3CN/H_2O V/V = 4:1	CO	-	98	-	10 h	2.72 s^{-1}	128
NiPor-CTF	0.5 $KHCO_3$	CO	0.9	~90	52.9	20 h	-	129
Ni SAs/NCNTs	0.5 $KHCO_3$	CO	-0.9	97	41.5	30 h	1176	69
Ni-N-C	0.1 $KHCO_3$ pH=6.8	CO	-1.2	90	12	10 h	-	91
Cu_2O/NRGO	0.1 $KHCO_3$	C_2H_4	-1.4	19.7	12	10000 s	-	130
Ni/Fe-N-C	0.5 $KHCO_3$	CO	-0.7	98	9.5	30 h	-	131
Fe-SA-900	0.1 $KHCO_3$	CO	-0.58	90	-	-	-	66
Ni/N-CHS	0.5 $KHCO_3$	CO	-0.9	93.1	17.1	16 h	-	132
(Cl, N)-Mn/G	0.5 $KHCO_3$	CO	0.49	97	13.4	-	38347	133
FeNPCN	0.1 $KHCO_3$	CO	-0.5	94	-	12 h	-	83
SA-Zn/MNC	1 $KHCO_3$	CH_4	-1.8	85	-31.8	35 h	-	95
Fe-N/CNT@GNR	0.1 $KHCO_3$	CO	-0.76	98	22.6	5 h	-	134
Fe-N-C	0.5 $KHCO_3$	CO	-0.5	95	1.9	-	-	135

3. Reaction Mechanism

In general, the process of catalytic CO_2 reduction can be expressed in Fig. 9. Firstly, CO_2 is absorbed and interacts with the active atoms of the catalyst to produce $*CO_2^-$, followed by the formation of intermediate products via various proton or electron transfer steps. Finally, desorption and formation of new products [136].

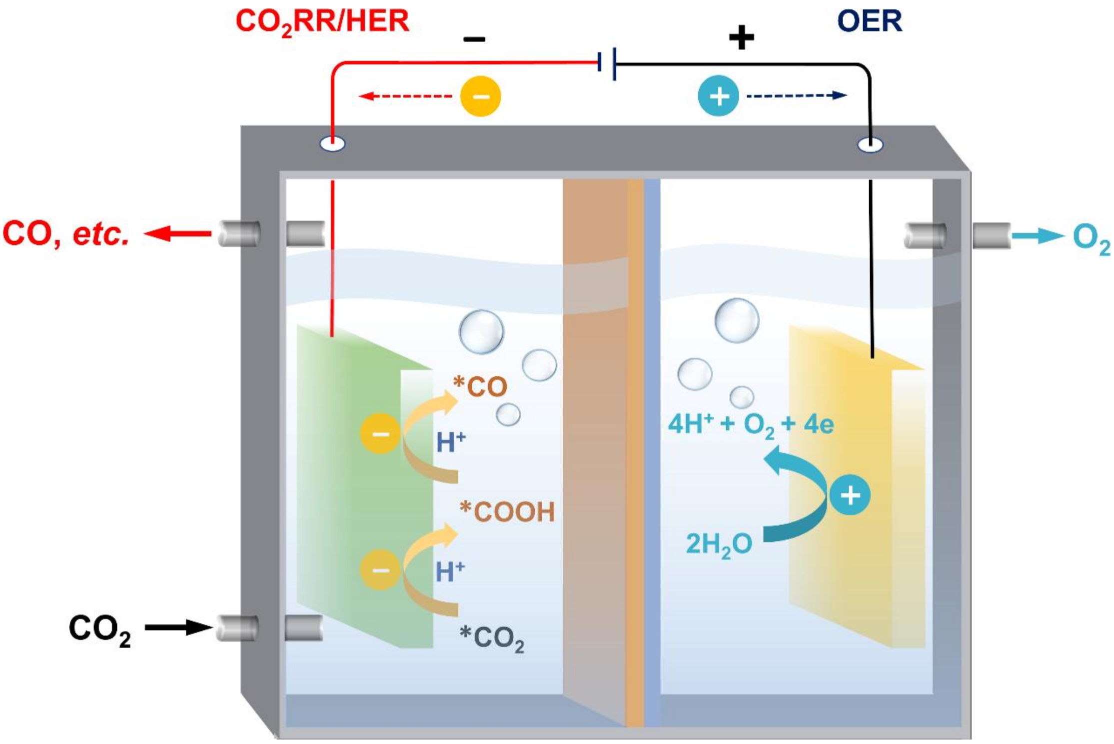

Fig. 9 The schematic diagram of electrochemical CO_2RR mechanism at M-N-Cs, where * stands for the active reaction sites.

For typical C1 products contain CO, CH_4, HCOOH, and CH_3OH (Fig. 10a). The first proton-coupled electron transfer (PCET) process can either form the intermediate product COOH* (top path) or OCHO* (bottom path) on different atoms [137, 138], followed by the second electrochemical step with two different paths which result in *CO and *HCOOH, respectively [76, 138]. Finally, CO or $HCOO^-$ is desorbed from the surface of the electrode as the final step [139]. Through experimental studies, it is widely accepted that *CO is an essential intermediate for the formation of CH_4, HCHO, and CH_3OH [140, 141]. DFT calculations indicated that the Cu [142-144] surface is thermodynamically conducive to the formation of initial *CO intermediates, followed by continuous hydrogenation to produce *CHO, *CH_2O, and *CH_3O. Finally, CH_4 is formed and the *O is converted to H_2O.

For C_2 and C_{2+} products, such as propanol(C_3H_7OH), ethanol(C_2H_5OH), acetaldehyde (CH_3CHO), and ethylene ($CH_2=CH_2$), *etc* [117, 145]. (Fig. 10b), it's generally proposed that the C-C bond is formed through two pathways [146]. One pathway indicates that *CO is first hydrogenated, followed by the proton transfer processes of *CHO [147]. In another pathway, the dimerization of *CO leads to the formation of the initial C-C coupling with the generation of *OCCO intermediates at low overpotentials [148, 149].

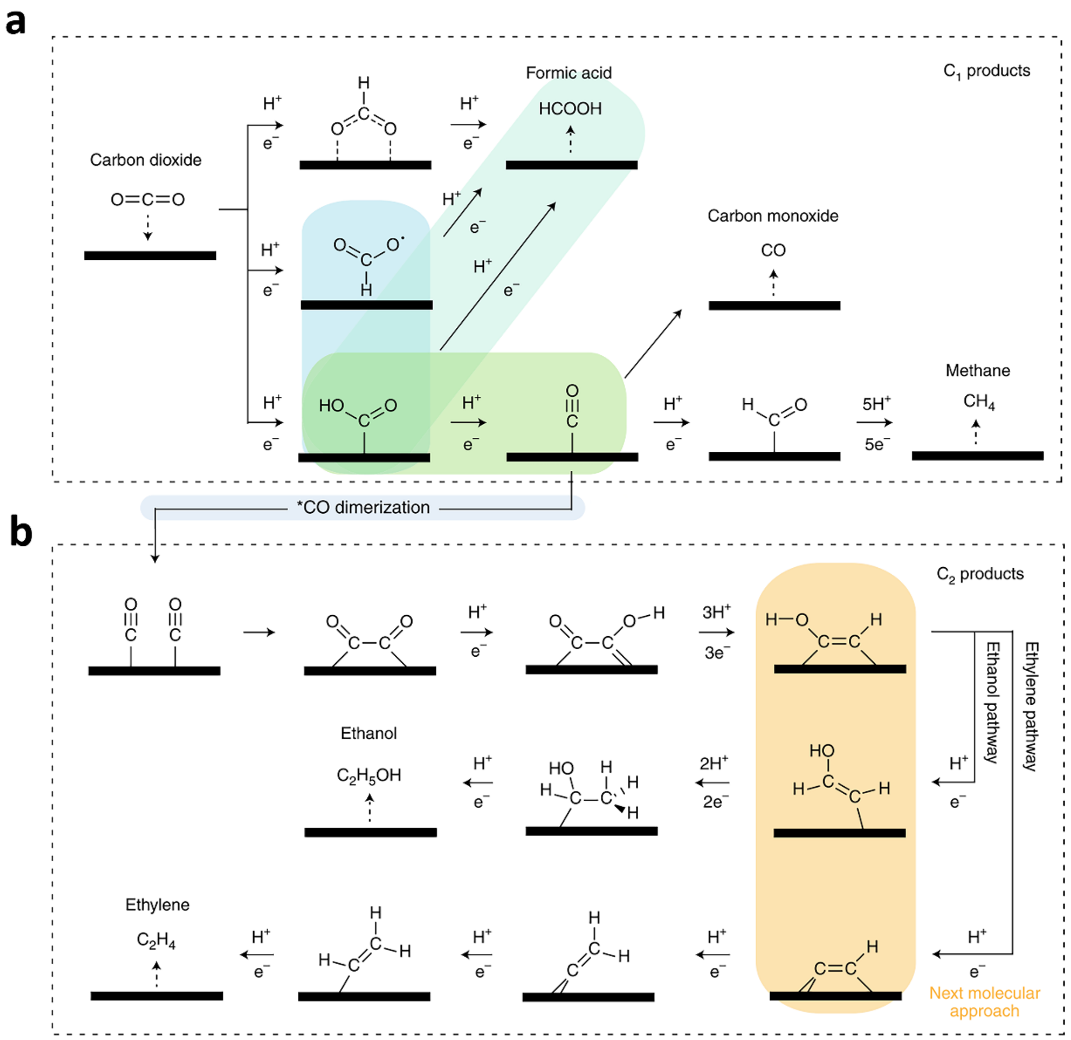

Fig. 10 (a-b) Reaction pathway for C_1 and C_2 products. Figure adapted with permission from Reference [149], Copyright © 2020, Springer Nature.

4. Active Sites

It's known to us that the CO_2RR process contains multiple proton/electron transfer steps, involving numerous intermediates and high energy barriers. Thus the real active sites during the reaction are still not clear. Up to now, there are three hypotheses were widely accepted. It has been proposed that adequately strong bonding between CO and the metal promotes the generation of CO and the generation of hydrocarbons [149]. Thus, the atomically dispersed metal centers were considered to be the active sites in M-N-Cs [74, 82, 87].

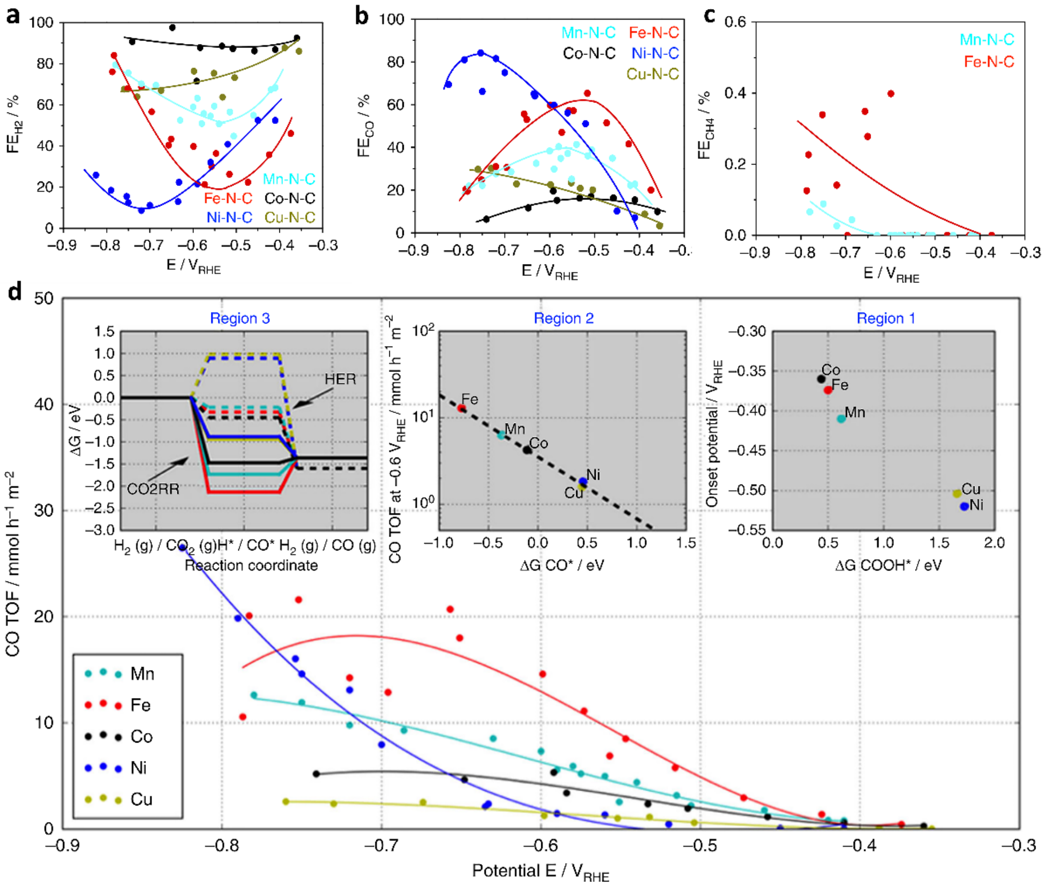

Fig. 11 (a-c) Faradaic Efficiencies (FE) of H_2, CO and CH_4, respectively. (d) Schematic diagram of the catalytic reactivity trends. Reproduced with permission from Reference [151], Copyright © 2017, Springer Nature.

Ju et al. [151] prepared a family of M-N-C electrocatalysts (M= Ni, Fe, Mn, Co, Cu) from bipyridine-based coordinated polymers, while discussing the effect of the active metal center on the CO_2RR. Finally, they found that the metal played the main role in comparison with other M-N_x functionalities through a series of theoretical calculations and studies. Considering Fig. 11a-c, it's clear that Co-N-C has poor selectivity towards CO_2RR. Whereas Fe-N-C, especially Ni-N-C catalysts, exhibit a better selectivity for

CO formation. Besides, Fe and Mn can lead to CO being further reduced to form traces of CH_4. Although activity can be judged via a single descriptor, such as current density, overpotential, *etc*., selectivity involves various factors due to complex reaction paths [9, 152]. And the different reduction paths depend on the applied potential and metal center. The specific turnover frequencies (TOF) of CO production trends for different M-N-C catalysts are shown in Fig. 11d. The result shows that the Ni-based catalysts exhibit a high CO selectivity and suppression of HER. This is because Ni-based catalysts possess favorable energetics for the CO_2RR, while having a very weak binding of *H. By contrast, Co-based catalysts with stronger *H adsorption display the highest Faradaic efficiency for HER, leading to a lower CO selectivity. The CO selectivity trend of other metal centers is as follows: Ni > Fe > Mn > Co = Cu. This is probably related to the binding strength of intermediates. For instance, Asset et al. [148] divide the M-N-C electrocatalysts into three main types according to the bonding strength between the metal with CO, (i) Ni, Zn, Cu belong to the “weak-CO binder”, (ii) Cr, Fe, Mn belong to the “strong-CO binder”, and (iii) Co-N-C belongs to a special category.

These results demonstrate the prospect of M-N-C catalysts as efficient CO_2RR catalyst alternatives to noble metal and emphasize the importance of the metal center on CO_2RR selectivity. Numerous studies have shown that M-N_4 (especially pyridine-N) centers are generally considered as possible active sites in these M-N-C structures [119, 153]. Li et al. [119] synthesized a Ni-N_4-C catalyst with a topo-chemical transformation method for CO_2 reduction. It was confirmed that the active site of Ni-N_4 improves selectivity and activity for CO_2RR.

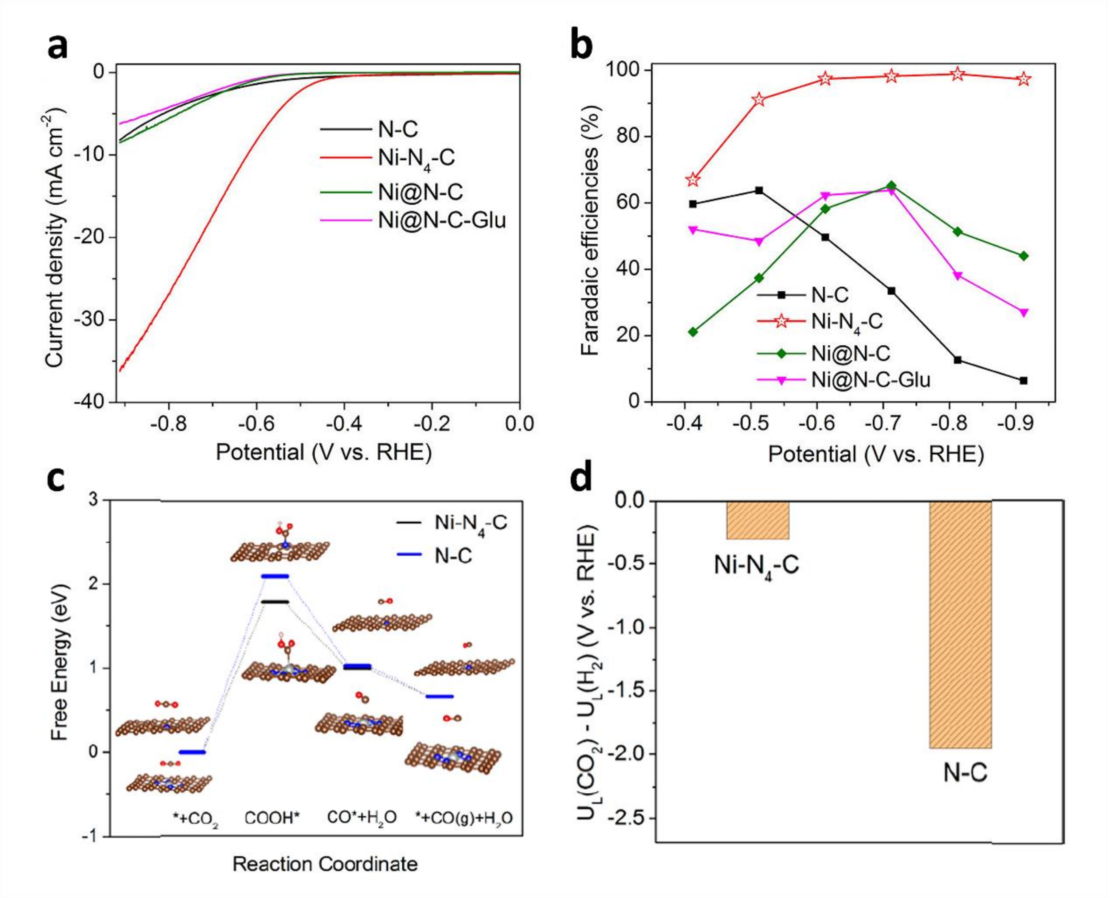

Fig. 12 (a) Current density-potential curves. (b) Faradaic efficiencies for CO. (c) Calculated free energy diagram. (d) The limiting potential difference between CO_2RR and HER. Reproduced with permission from Reference [119], Copyright © 2017 American Chemical Society.

As seen in Fig. 12a, Ni-N_4-C exhibits excellent activity compared with N-C in the electrolyte. In contrast, despite the existence of Ni, the CO_2RR performance of Ni@N-C and Ni@N-C-Glu prepared directly by pyrolysis are poor, demonstrating the advantage of Ni-N_4-C. Besides, the Ni-N_4-C exhibits near 100% Faraday efficiency (Fig. 12b). The calculated free energy diagrams for CO_2RR by density functional theory (DFT) indicated that the COOH*, an adsorbed intermediate, was the rate-determining step for both Ni-N_4-C and N-C (Fig. 12c). Compared with N-C, the presence of Ni-N_4 site reduced the generation energy of COOH* and promoted the generation of CO, thus showing higher activity. As seen in Fig. 12d, the limiting potential difference of Ni-N_4-C is larger than that of N-C, indicating that Ni-N_4-C has a high selectivity for CO_2 conversion to CO. Combining thermodynamical DFT with experimental analysis, it is found that Ni-N_4 structure has good catalytic activity and selectivity, which can reduce the energy barrier of CO_2RR and accelerate charge transfer.

However, the precise nature of the active centers is still controversial as there are several reported possibilities, such as other N structures and even a C site directly adjoining an N site [154-156]. This is because under the high-temperature synthesis for the M-N-C electrocatalysts, the resulting products tend to form complicated M-N_x (x = 1-4), M-C_x, or defects in the carbon matrix.

5. The strategies for optimizing the materials of SACs

Current research to obtain high-performance M-N-C electrocatalysts can be summarised as having three strategies:

(i) Increasing the density of active sites [32]. One strategy to such a target is to use precursors containing high nitrogen content [123, 157]. Only when the content of nitrogen in the precursors is high, it’s possible to obtain heavily loaded atomically dispersed M-N_x motifs which were considered as active sites. Another solution is to make full use of the space confinement effect to restrain the agglomeration of metal atoms and enhance the metal-atom utilization [8, 108, 158]. The research group of Professor Luo and Fu [159] successfully realized the preparation of a new type of self-supporting electrode with ultra-thin carbon nanosheets and ultra-fine Bi nanoparticles by annealing the impregnated carbon cloth in one step. Owing to the uniformly distributed ultrafine Bi particles and the carbon nanosheets formed by in-situ annealing, the optimized electrode not only exhibits high formic acid selectivity in the process of reducing CO_2, but also exhibits excellent catalytic activity and stability. Professor Jin's team [160] used the principle of Rayleigh instability to construct a “drop-tube” one-dimensional hollow structure of Bi nanorod@N-doped carbon nanotubes (Bi-NRs@NCNTs) composite catalyst, under a low overpotential, it can convert CO_2 into formate products with high selectivity. In addition, after 24 hours of continuous long-term electrocatalytic testing, Bi-NRs@NCNTs can still maintain good activity and stability.

(ii) Improving the intrinsic performance of active sites [24]. As is well-known, an ideal catalyst should have a moderate interaction with reactive species, neither too strong nor too weak. Thus, adjusting the electronic structures of active metal-atom centers can effectively improve the intrinsic catalytic performance [161]. Because the adsorption behavior of a catalyst depends on the electronic structures of active sites. Thus, there are the following four strategies to effectively alter the d-orbital chemistry of central metal ions. 1) selecting the optimal metal center ions with moderate surface adsorption behavior [82]; 2) bringing in other heteroatoms into the carbon skeleton to tune the electron structure of carbon materials, such as N, S, B, *etc.* [107, 108, 162-165] For instance, Wang et al. [166] prepared N-doped porous carbon polyhedra containing trace Fe atoms (Fe_1NC) by gas diffusion and one-step thermal activation method, the optimized catalyst showed good CO_2RR performance with CO Faraday efficiency as high as 96%, and excellent stability, which is attributed to the greatly improved accessibility and intrinsic activity of the active centers, due to an increase in the electrochemical surface area through dimensional modulation and the redistribution of doped N species through thermal activation. 3) adjusting the coordination environment of central metal ions, such as the coordination number and coordinated atoms, without changing the dispersion of a single atom, thus establishing the relationship among the coordination environment, electronic structure, and catalytic performance of a single atom [167-169]; using MOFs without N as precursors, Jiang et al. [156] proposed a universal host-guest coordination protection strategy to prepare a series of SACs, and successfully realized the highly selective conversion of CO_2 to CO by regulating the coordination environment of monoatomic Ni catalysts. Theoretical calculations show that the low N coordination number of single-atom Ni sites is beneficial to the formation of COOH* intermediates, thereby improving its catalytic activity. Yan et al. [44] successfully prepared a porous carbon material doped with coordinated unsaturated Ni-N sites by pyrolyzing the zinc/nickel bimetallic zeolite imidazole framework material (ZIF-8), and achieved the high-efficiency electrocatalytic conversion of CO_2. 4) construct the diatomic metal active sites or single atomic nanoarrays, which can further improve catalytic activity through strong coupling synergies and enhanced charge transfer performance [133, 157, 170, 171]. The research work of diatomic catalysts reported so far mainly focuses on two aspects: homonuclear metal diatomic catalysts [172-174] and heteronuclear metal diatomic catalysts [131, 175, 176]. Xing et al. [173] used the organometallic framework as the precursor, and accurately prepared the diatomic center catalyst with high active structure by adjusting the content of active component Co. The activity increased by more than one order of magnitude, reaching 13 times of the current single atomic active site catalyst. The existence of the active site structure of the diatomic Co center was confirmed by spherical aberration correction electron microscopy and extended X-ray absorption near edge spectrum. The heteronuclear diatomic catalyst can more effectively regulate the central position of the *d*-band through the synergistic action of different metals, thus optimizing the interaction between the reactants or intermediates and the catalytic active site, which leads to high catalytic activity. Ren et al. [131] achieved isolated diatomic Ni/Fe sites anchored on

N-doped carbon (Ni/Fe-N_6-C), which could serve as an efficient electrocatalyst for the reduction of CO_2 to CO. The excellent performance can be attributed to the charge transfer and redistribution caused by the electronegativity difference between the heteronuclear bimetallic atoms, thereby optimizing the adsorption and desorption process of reaction intermediates. In order to deeply understand the structural characteristics of bimetallic site catalysts, Luo et al. [176] used density functional theory calculations and micro-kinetic simulations to study the adsorption characteristics and catalytic performance of a series of potential bimetallic sites for CO_2 reduction reactions. Using the adsorption strength of OH* and COOH* intermediates as descriptors, they obtained three potential bimetallic site catalysts, namely Ni/Fe, Ni/Mn, and Cu/Mn, through two rounds of screening. Studies have found that in these three bimetallic site catalysts, the linear relationship between COOH* and CO* adsorption energy is broken, which leads to their excellent CO_2 reduction activity. In addition, self-supporting monoatomic nano-arrays with catalytically active components directly grown on three-dimensional substrates (such as carbon cloth, nickel foam) is also a good way to improve the intrinsic activity of the catalyst because of their unique porous structure, high density of active sites, improved mass transfer, enhanced charge conduction, and excellent electrocatalytic activity.

(iii) Optimizing the reaction conditions after understanding the influence of structure and material composition on its reactivity. Particularly the type of electrolyte can greatly influence the formation of absorbed intermediates and rate-determining steps [177-179]. Aqueous electrolytes contain a large number of metal cations and inorganic anions, which affect the selectivity and current density of CO_2RR products.

Singh et al. [178] discussed the influence of electrolyte cation size on CO_2RR. The result confirmed that the pK_a of cation hydrolysis reduces with an increase of cation size, which is low enough to act as a buffering solution. Buffering reduces the pH near the cathode and increases the local concentration of dissolved CO_2. Those changes facilitate the increase of cathode activity, resulting in the decrease of Faraday efficiency of H_2 and CH_4, while the increase of Faraday efficiency of CO, C_2H_4 and C_2H_5OH, as shown in Fig. 13.

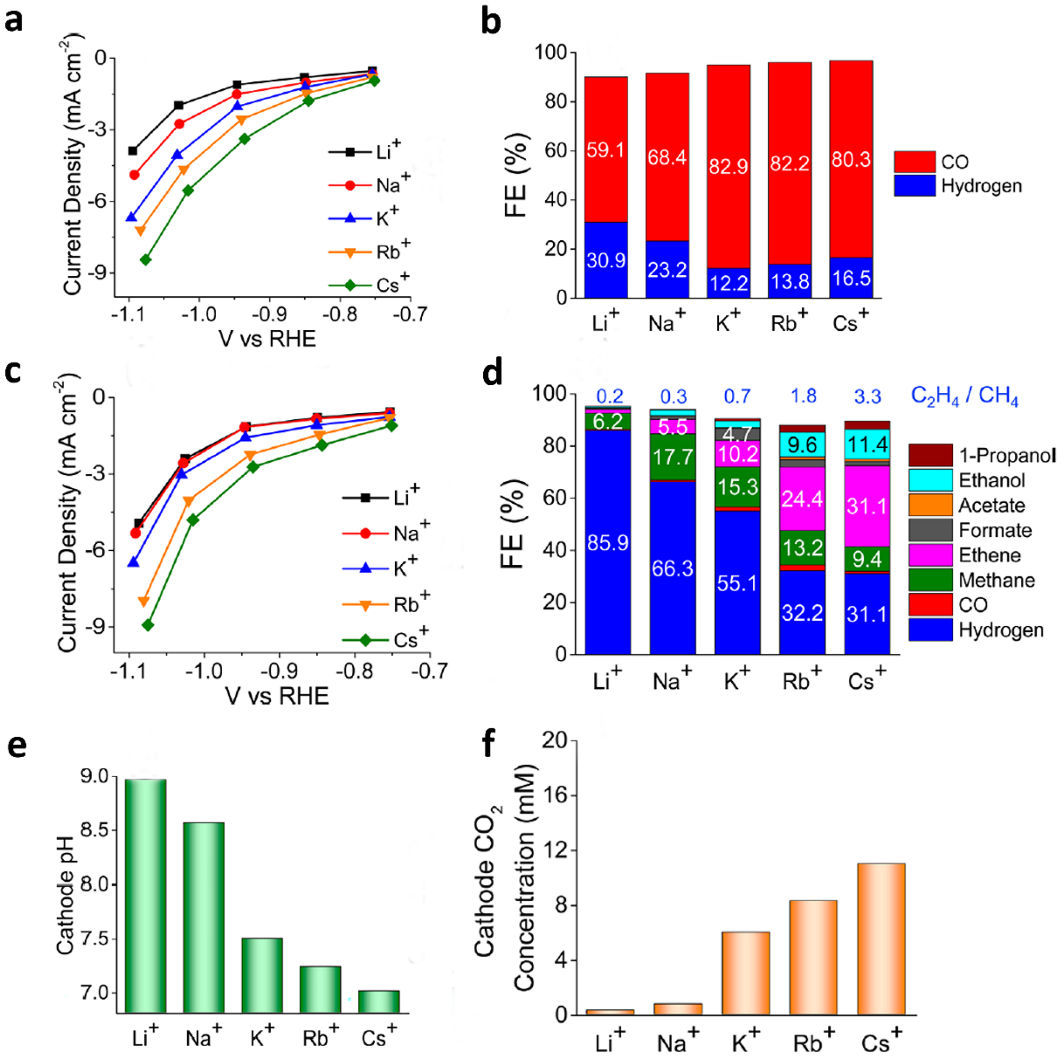

Fig. 13 (a) Linear sweep voltammetric curves on Ag cathode, (b) corresponding Faradaic efficiency at applied potential -1 V *vs.* RHE, (c) linear sweep voltammetric curves on Cu cathode, and (d) corresponding Faradaic efficiency at applied potential -1 V *vs.* RHE. Calculated values of (e) cathode pH, (f) cathode CO_2 concentration.

Reproduced with permission from Reference [178], Copyright © 2016 American Chemical Society.

6. Summary and Outlook

In recent years, transition metal-nitrogen-carbon catalysts (M-N-C) have emerged as an inexpensive alternative for preparing high-performance CO_2RR electrocatalysts. Especially, the Faradaic selectivity of Ni-based catalysts to CO can reach 99% and Fe containing N-doped porous carbon materials can reduce CO to CH_4. To obtain catalysts with highly active, selective, and long-term stability, efforts are required to find optimal reaction conditions. For instance, optimal metal center, suitable carbon support, temperature, pH, mass loading, and heteroatom doping.

However, when the metal particles are reduced to the single-atom level, the specific surface area increases sharply, leading to a sharp increase in the free energy of the metal surface. During the preparation and reaction, agglomeration coupling is very easy to form large clusters, which leads to the deactivation of the catalyst. Therefore, stability and loading capacity are the great challenges faced by the single-atom catalysts (SACs).

Low mass loading of SACs greatly limits the current density, thus affecting practical applications. However, increasing the loading capacity is bound to face the problem of atom migration and agglomeration to form nanoparticles. Thus we have to keep the balance between loading and catalytic performance. Therefore, in terms of synthesis, the following aspects are needed for considering: (1) select the appropriate metal center based on the volcano-like relationship between the key free energy of adsorption and catalytic activity; (2) through space restriction, defect trapping, coordination anchoring and other effective means to achieve the dispersion and separation of the atom which inhibit its migration and aggregation on the carrier; (3) Stabilize a single metal atom on the carrier by enhancing the metal-carrier interaction; (4) from the functional design of the carrier as an entry point to regulate the performance of single-atom catalytic materials, make it achieve synergistic catalysis with the carrier, and improve the performance of the catalyst; (5) precisely control the coordination environment of metal atoms to optimize the local electronic structure and improve the catalytic performance of SACs.

In addition, a uniform active site is still difficult to achieve, and the state of the active site during the reaction is still unclear. The information we know about the active site of M-N-Cs is still not enough to design an appropriate structure for each specific reaction. Therefore, more efforts are needed to determine the active site, and some major challenges and research topics that have not been fully studied are noted:

(1) Choosing single-atom catalyst as a model system, using in-situ electron microscopy or in-situ synchrotron radiation and other in-situ characterization methods to observe and track the reaction process, combined with theoretical calculations to study the structure-activity relationship between its structure and catalytic performance, and to explore catalytic reactions mechanism. To achieve the precise synthesis of active site catalysts, and the maximum ability of each atom can be used to promote the reaction.

(2) More coordination environments need to be developed for M-N-C. So far, coordination atoms are usually nonmetallic elements including C, N, O, S, and so on. Compared with other structures such as metal compounds and alloys, the adjustable space of the structure of M-N-C is relatively limit, which restricts its application in certain situations. Therefore, substituting other metal elements for non-metallic elements or constructing active sites of heteroatoms (M_1M_2-N-C) is a new opportunity,

which not only leads to more coordination environment combinations but also could result in synergy between two adjacent metal atoms on the active site.

(3) Improve catalytic performance based on engineering external factors. For example, strain engineering has been proven to be an effective way to improve the catalytic activity of catalysts [180-182]. Strain can be achieved by mechanical loading or heterostructure lattice mismatch, and the heterostructure can continuously adjust the *d*-band width and center of the metal catalyst and molecular surface interaction. Biaxial or anisotropic strain can also be used to achieve anisotropic modulation of the binding energy of different species on the MNC catalyst, thereby changing the adsorption/desorption behavior of reactants or intermediates on the catalyst. In addition, some external factors, such as magnetic field, electric field, confinement effect, solvent effect, etc., can adjust the adsorption of intermediates on the catalyst to varying degrees. Due to the different physical and/or chemical properties of the adsorbates involved, this also benefits to improve the activity and selectivity of the target product.

In conclusion, the key to the overall catalytic performance of the ideal material is not an independent issue. The superior catalytic performance of M-N-C-based materials can only be achieved through a combination of a series of design strategies, such as adjusting the properties of the metal ion center, reaction conditions, coordination environment, carbon support, and mass loading, as discussed in this review. Similarly, turning CO_2 into high value-added liquid fuels and chemical products has huge potential but faces substantial technological challenges that require a multi-disciplinary approach, with materials science playing a central role. We hope that the design principles and methods of metal nitrogen-doped carbon single-atom electrocatalysts proposed in this review will help design new high-performance catalysts that can better meet the needs of industrial applications.

7. Acknowledgments

The authors gratefully acknowledge financial supports by the National Natural Science Foundation of China (51602193, 21703267), Startup Fund for Youngman Research at SJTU, the Foundation Research Project of Jiangsu Province (BK20170423), the STFC Batteries Network (ST/R006873/1), and EPSRC (EP/R023581/1, EP/P009050/1, EP/V027433/1).

References

[1] C.D. Allen, A.K. Macalady, H. Chenchouni, D. Bachelet, N. McDowell, M. Vennetier, T. Kitzberger, A. Rigling, D.D. Breshears, E.H. Hogg, P. Gonzalez, R. Fensham, Z. Zhang, J. Castro, N. Demidova, J.-H. Lim, G. Allard, S.W. Running, A. Semerci, N. Cobb, A global overview of drought and heat-induced tree mortality reveals emerging climate change risks for forests, Forest Ecol. Manag. 259 (2010) 660-684.

[2] B. Obama, The irreversible momentum of clean energy, Science 355 (2017) 126-129.

[3] D. McCollum, N. Bauer, K. Calvin, A. Kitous, K. Riahi, Fossil resource and energy security dynamics in conventional and carbon-constrained worlds, Climatic Change 123 (2013) 413-426.

[4] S. Chu, A. Majumdar, Opportunities and challenges for a sustainable energy future, Nature 488 (2012) 294-303.

[5] S. Chu, Y. Cui, N. Liu, The path towards sustainable energy, Nat. Mater. 16 (2016) 16-22.

[6] C. Song, Global challenges and strategies for control, conversion and utilization of CO_2 for sustainable development involving energy, catalysis, adsorption and chemical processing, Catal. Today 115 (2006) 2-32.

[7] R.J. Lim, M. Xie, M.A. Sk, J.-M. Lee, A. Fisher, X. Wang, K.H. Lim, A review on the electrochemical reduction of CO_2 in fuel cells, metal electrodes and molecular catalysts, Catal. Today 233 (2014) 169-180.

[8] Y. Cheng, S. Zhao, B. Johannessen, J.P. Veder, M. Saunders, M.R. Rowles, M. Cheng, C. Liu, M.F. Chisholm, R. De Marco, H.M. Cheng, S.Z. Yang, S.P. Jiang, Atomically dispersed transition metals on carbon nanotubes with ultrahigh loading for selective electrochemical carbon dioxide reduction, Adv. Mater. 30 (2018) 1706287.

[9] M.B. Ross, P. De Luna, Y. Li, C.-T. Dinh, D. Kim, P. Yang, E.H. Sargent, Designing materials for electrochemical carbon dioxide recycling, Nat. Catal. 2 (2019) 648-658.

[10] Y.Y. Birdja, E. Pérez-Gallent, M.C. Figueiredo, A.J. Göttle, F. Calle-Vallejo, M.T.M. Koper, Advances and challenges in understanding the electrocatalytic conversion of carbon dioxide to fuels, Nat. Energy 4 (2019) 732-745.

[11] P. Prabhu, V. Jose, J.M. Lee, Heterostructured catalysts for electrocatalytic and photocatalytic carbon dioxide reduction, Adv. Funct. Mater. 30 (2020) 1910768.

[12] A. Bagger, W. Ju, A.S. Varela, P. Strasser, J. Rossmeisl, Electrochemical CO_2 reduction: A classification problem, Chemphyschem 18 (2017) 3266-3273.

[13] T. Hatsukade, K.P. Kuhl, E.R. Cave, D.N. Abram, T.F. Jaramillo, Insights into the electrocatalytic reduction of CO_2 on metallic silver surfaces, Phys. Chem. Chem. Phys. 16 (2014) 13814-13819.

[14] H. Wang, J. Li, K. Li, Y. Lin, J. Chen, L. Gao, V. Nicolosi, X. Xiao, J.M. Lee, Transition metal nitrides for electrochemical energy applications, Chem. Soc. Rev. 50 (2021) 1354-1390.

[15] Y. Chen, C.W. Li, M.W. Kanan, Aqueous CO_2 reduction at very low overpotential on oxide-derived Au nanoparticles, J. Am. Chem. Soc. 134 (2012) 19969-19972.

[16] Z.W. Seh, J. Kibsgaard, C.F. Dickens, I. Chorkendorff, J.K. Norskov, T.F. Jaramillo, Combining theory and experiment in electrocatalysis: Insights into materials design, Science 355 (2017) eaad4998.

[17] J.-P. Jones, G.K.S. Prakash, G.A. Olah, Electrochemical CO_2 reduction: Recent advances and current trends, Isr. J. Chem. 54 (2014) 1451-1466.

[18] Y. Xiong, J. Dong, Z.Q. Huang, P. Xin, W. Chen, Y. Wang, Z. Li, Z. Jin, W. Xing, Z. Zhuang, J. Ye, X. Wei, R. Cao, L. Gu, S. Sun, L. Zhuang, X. Chen, H. Yang, C. Chen, Q. Peng, C.R. Chang, D. Wang, Y. Li, Single-atom Rh/N-doped carbon electrocatalyst for formic acid oxidation, Nat. Nanotechnol. 15 (2020) 390-397.

[19] A. Beniya, S. Higashi, N. Ohba, R. Jinnouchi, H. Hirata, Y. Watanabe, CO oxidation activity of non-reducible oxide-supported mass-selected few-atom Pt single-clusters, Nat. Commun. 11 (2020) 1888.

[20] K.P. Kuhl, T. Hatsukade, E.R. Cave, D.N. Abram, J. Kibsgaard, T.F. Jaramillo, Electrocatalytic conversion of carbon dioxide to methane and methanol on transition metal surfaces, J. Am. Chem. Soc. 136 (2014) 14107-14113.

[21] P. Prabhu, V. Jose, J.-M. Lee, Design strategies for development of TMD-based heterostructures in electrochemical energy systems, Matter 2 (2020) 526-553.

[22] G. Fu, J.-M. Lee, Ternary metal sulfides for electrocatalytic energy conversion, J. Mater. Chem. A 7 (2019) 9386-9405.

[23] H. Wang, J.-M. Lee, Recent advances in structural engineering of MXene electrocatalysts, J. Mater. Chem. A 8 (2020) 10604-10624.

[24] Y. Jiao, Y. Zheng, P. Chen, M. Jaroniec, S.Z. Qiao, Molecular scaffolding strategy with synergistic active centers to facilitate electrocatalytic CO_2 reduction to hydrocarbon/alcohol, J. Am. Chem. Soc. 139 (2017) 18093-18100.

[25] A.S. Varela, W. Ju, P. Strasser, Molecular nitrogen–carbon catalysts, solid metal organic framework catalysts, and solid metal/nitrogen-doped carbon (MNC) catalysts for the electrochemical CO_2 reduction, Adv. Energy Mater. 8 (2018) 1703614.

[26] K. Elouarzaki, V. Kannan, V. Jose, H.S. Sabharwal, J.M. Lee, Recent trends, benchmarking, and challenges of electrochemical reduction of CO_2 by molecular catalysts, Adv. Energy Mater. 9 (2019) 1900090.

[27] Y. Zheng, P. Cheng, J. Xu, J. Han, D. Wang, C. Hao, H.R. Alanagh, C. Long, X. Shi, Z. Tang, MOF-derived nitrogen-doped nanoporous carbon for electroreduction of CO_2 to CO: the calcining temperature effect and the mechanism, Nanoscale 11 (2019) 4911-4917.

[28] H.B. Wu, X.W.D. Lou, Metal-organic frameworks and their derived materials for electrochemical energy storage and conversion: Promises and challenges, Sci. Adv. 3 (2017) eaap9252.

[29] J.M. Falkowski, S. Liu, W. Lin, Metal-organic frameworks as single-site solid catalysts for asymmetric reactions, Isr. J. Chem. 52 (2012) 591-603.

[30] B. Kumar, M. Asadi, D. Pisasale, S. Sinha-Ray, B.A. Rosen, R. Haasch, J. Abiade, A.L. Yarin, A. Salehi-Khojin, Renewable and metal-free carbon nanofibre catalysts for carbon dioxide reduction, Nat. Commun. 4 (2013) 2819.

[31] A. Vasileff, Y. Zheng, S.Z. Qiao, Carbon solving carbon's problems: Recent progress of nanostructured carbon-based catalysts for the electrochemical reduction of CO_2, Adv. Energy Mater. 7 (2017) 1700759.

[32] P. Xia, M. Antonietti, B. Zhu, T. Heil, J. Yu, S. Cao, Designing defective crystalline carbon nitride to enable selective CO_2 photoreduction in the gas phase, Adv. Funct. Mater. 29 (2019) 1900093.

[33] X. Cui, Z. Pan, L. Zhang, H. Peng, G. Zheng, Selective etching of nitrogen-doped carbon by steam for enhanced electrochemical CO_2 reduction, Adv. Energy Mater. 7 (2017) 1701456.

[34] Z. Han, C. Choi, H. Tao, Q. Fan, Y. Gao, S. Liu, A.W. Robertson, S. Hong, Y. Jung, Z. Sun, Tuning the Pd-catalyzed electroreduction of CO_2 to CO with reduced overpotential, Catal. Sci. Technol. 8 (2018) 3894-3900.

[35] S.C. Abeyweera, J. Yu, J.P. Perdew, Q. Yan, Y. Sun, Hierarchically 3D porous Ag nanostructures derived from silver benzenethiolate nanoboxes: Enabling CO_2 reduction with a near-unity selectivity and mass-specific current density over 500 A/g, Nano Lett. 20 (2020) 2806-2811.

[36] W. Zhu, R. Michalsky, O. Metin, H. Lv, S. Guo, C.J. Wright, X. Sun, A.A. Peterson, S. Sun, Monodisperse Au nanoparticles for selective electrocatalytic reduction of CO_2 to CO, J. Am. Chem. Soc. 135 (2013) 16833-16836.

[37] D. Huang, Y. Luo, S. Li, L. Liao, Y. Li, H. Chen, J. Ye, Recent advances in tuning the electronic structures of atomically dispersed M-N-C materials for efficient gas-involving electrocatalysis, Mater. Horiz. 7 (2020) 970-986.

[38] H. Liu, Y. Zhu, J. Ma, Z. Zhang, W. Hu, Recent advances in atomic-level engineering of nanostructured catalysts for electrochemical CO_2 reduction, Adv. Funct. Mater. 30 (2020) 1910534.

[39] J. Su, R. Ge, Y. Dong, F. Hao, L. Chen, Recent progress in single-atom electrocatalysts: concept, synthesis, and applications in clean energy conversion, J. Mater. Chem. A 6 (2018) 14025-14042.

[40] S. Back, J. Lim, N.Y. Kim, Y.H. Kim, Y. Jung, Single-atom catalysts for CO_2 electroreduction with significant activity and selectivity improvements, Chem. Sci. 8 (2017) 1090-1096.

[41] H. Ou, D. Wang, Y. Li, How to select effective electrocatalysts: Nano or single atom?, Nano Select 2 (2020) 492-511.

[42] C. Zhu, S. Fu, Q. Shi, D. Du, Y. Lin, Single-atom electrocatalysts, Angew.Chem.Int.Ed. 56 (2017) 13944-13960.

[43] Y. Chen, S. Ji, C. Chen, Q. Peng, D. Wang, Y. Li, Single-atom catalysts: Synthetic strategies and electrochemical applications, Joule 2 (2018) 1242-1264.

[44] C. Yan, H. Li, Y. Ye, H. Wu, F. Cai, R. Si, J. Xiao, S. Miao, S. Xie, F. Yang, Y. Li, G. Wang, X. Bao, Coordinatively unsaturated nickel-nitrogen sites towards selective and high-rate CO_2 electroreduction, Energy Environ. Sci. 11 (2018) 1204-1210.

[45] X. Duan, J. Xu, Z. Wei, J. Ma, S. Guo, S. Wang, H. Liu, S. Dou, Metal-free carbon materials for CO_2 electrochemical reduction, Adv. Mater. 29 (2017) 1701784.

[46] K. Leung, I.M.B. Nielsen, N. Sai, C. Medforth, J.A. Shelnutt, Cobalt-porphyrin catalyzed electrochemical reduction of carbon dioxide in water. 2. mechanism from first principles, J. Phys. Chem. A 114 (2010) 10174-10184.

[47] A. Bagger, W. Ju, A.S. Varela, P. Strasser, J. Rossmeisl, Single site porphyrine-like structures advantages over metals for selective electrochemical CO_2 reduction, Catal. Today 288 (2017) 74-78.

[48] T. Zheng, K. Jiang, H. Wang, Recent advances in electrochemical CO_2-to-CO conversion on heterogeneous catalysts, Adv. Mater. 30 (2018) 1802066.

[49] D.D. Zhu, J.L. Liu, S.Z. Qiao, Recent advances in inorganic heterogeneous electrocatalysts for reduction of carbon dioxide, Adv. Mater. 28 (2016) 3423-3452.

[50] C. Gao, J. Low, R. Long, T. Kong, J. Zhu, Y. Xiong, Heterogeneous single-atom photocatalysts: Fundamentals and applications, Chem. Rev. 120 (2020) 12175-12216.

[51] T. Maschmeyer, F. Rey, G. Sankar, J.M. Thomas, Heterogeneous catalysts obtained by grafting metallocene complexes onto mesoporous silica, Nature 378 (1995) 159-162.

[52] B. Qiao, A. Wang, X. Yang, L.F. Allard, Z. Jiang, Y. Cui, J. Liu, J. Li, T. Zhang, Single-atom catalysis of CO oxidation using Pt_1/FeO_x, Nat. Chem. 3 (2011) 634-41.

[53] U. Heiz, A. Sanchez, S. Abbet, W.-D. Schneider, Catalytic oxidation of carbon monoxide on monodispersed platinum clusters: Each atom counts, J. Am. Chem. Soc. 121 (1999) 3214-3217.

[54] S. Abbet, A. Sanchez, U. Heiz, W.-D. Schneider, A.M. Ferrari, G. Pacchioni, N. Ro1sch, Acetylene cyclotrimerization on supported size-selected Pd_n clusters ($1< n < 30$): One atom is enough!, J. Am. Chem. Soc. 122 (2000) 3453-3457.

[55] W.E. Kaden, T. Wu, W.A. Kunkel, S.L. Anderson, Electronic structure controls reactivity of size-selected Pd clusters adsorbed on TiO_2 surfaces, Science 326 (2009) 826-829.

[56] B.J. O'Neill, D.H.K. Jackson, J. Lee, C. Canlas, P.C. Stair, C.L. Marshall, J.W. Elam, T.F. Kuech, J.A. Dumesic, G.W. Huber, Catalyst design with atomic layer deposition, ACS Catal. 5 (2015) 1804-1825.

[57] H. Yan, H. Cheng, H. Yi, Y. Lin, T. Yao, C. Wang, J. Li, S. Wei, J. Lu, Single-atom Pd_1/graphene catalyst achieved by atomic layer deposition: Remarkable performance in selective hydrogenation of 1,3-butadiene, J. Am. Chem. Soc. 137 (2015) 10484-10487.

[58] F. Lü, H. Bao, Y. Mi, Y. Liu, J. Sun, X. Peng, Y. Qiu, L. Zhuo, X. Liu, J. Luo, Electrochemical CO_2 reduction: from nanoclusters to single atom catalysts, Sustainable Energy Fuels 4 (2020) 1012-1028.

[59] H. Wei, X. Liu, A. Wang, L. Zhang, B. Qiao, X. Yang, Y. Huang, S. Miao, J. Liu, T. Zhang, FeO_x-supported platinum single-atom and pseudo-single-atom catalysts for chemoselective hydrogenation of functionalized nitroarenes, Nat. Commun. 5 (2014) 5634.

[60] J.H. Kwak, L. Kovarik, J. Szanyi, Heterogeneous catalysis on atomically dispersed supported metals: CO_2 reduction on multifunctional Pd catalysts, ACS Catal. 3 (2013) 2094-2100.

[61] L. Lin, W. Zhou, R. Gao, S. Yao, X. Zhang, W. Xu, S. Zheng, Z. Jiang, Q. Yu, Y.W. Li, C. Shi, X.D. Wen, D. Ma, Low-temperature hydrogen production from water and methanol using Pt/α-MoC catalysts, Nature 544 (2017) 80-83.

[62] C. Zhu, S. Fu, J. Song, Q. Shi, D. Su, M.H. Engelhard, X. Li, D. Xiao, D. Li, L. Estevez, D. Du, Y. Lin, Self-assembled Fe-N-doped carbon nanotube aerogels with single-atom catalyst feature as high-efficiency oxygen reduction electrocatalysts, Small 13 (2017) 1603407.

[63] K. Hiratsuka, K. Takahashi, H. Sasaki, S. Toshima, Electrocatalytic behavior of tetrasulfonated metal phthalocyanines in the reduction of carbon dioxide, Chem. Lett. 6 (1977) 1137-1140.

[64] K. Hiratsuka, K. Takahashi, H. Sasaki, S. Toshima, Electrocatalytic behavior of metal porphyrins in the reduction of carbon dioxide, Chem. Lett. 8 (1979) 305-308.

[65] A.S. Varela, W. Ju, A. Bagger, P. Franco, J. Rossmeisl, P. Strasser, Electrochemical reduction of CO_2 on metal-nitrogen-doped carbon catalysts, ACS Catal. 9 (2019) 7270-7284.

[66] C. Xu, A. Vasileff, D. Wang, B. Jin, Y. Zheng, S.-Z. Qiao, Synergistic catalysis between atomically dispersed Fe and a pyrrolic-N-C framework for CO_2 electroreduction, Nanoscale Horiz. 4 (2019) 1411-1415.

[67] Y. Qu, Z. Li, W. Chen, Y. Lin, T. Yuan, Z. Yang, C. Zhao, J. Wang, C. Zhao, X. Wang, F. Zhou, Z. Zhuang, Y. Wu, Y. Li, Direct transformation of bulk copper into copper single sites via emitting and trapping of atoms, Nat. Catal. 1 (2018) 781-786.

[68] X. Han, X. Ling, Y. Wang, T. Ma, C. Zhong, W. Hu, Y. Deng, Generation of nanoparticle, atomic-cluster, and single-atom cobalt catalysts from zeolitic imidazole frameworks by spatial isolation and their use in zinc-air batteries, Angew. Chem. Int. Ed. 58 (2019) 5359-5364.

[69] P. Lu, Y. Yang, J. Yao, M. Wang, S. Dipazir, M. Yuan, J. Zhang, X. Wang, Z. Xie, G. Zhang, Facile synthesis of single-nickel-atomic dispersed N-doped carbon framework for efficient electrochemical CO_2 reduction, Applied Catalysis B: Environmental 241 (2019) 113-119.

[70] Z. He, K. He, A.W. Robertson, A.I. Kirkland, D. Kim, J. Ihm, E. Yoon, G.D. Lee, J.H. Warner, Atomic structure and dynamics of metal dopant pairs in graphene, Nano Lett. 14 (2014) 3766-3772.

[71] J. Li, S. Chen, N. Yang, M. Deng, S. Ibraheem, J. Deng, J. Li, L. Li, Z. Wei, Ultrahigh-loading zinc single-atom catalyst for highly efficient oxygen reduction in both acidic and alkaline media, Angew. Chem. Int. Ed. 58 (2019) 7035-7039.

[72] Y. hori, H. Wakebe, T. Tsukamoto, O. Koga, Electrocatalytic process of CO selectivity in electrochemical reduction of CO_2 at metal electrodes in aqueous media, Electrochim. Acta 39 (1994) 1833-1839.

[73] X. Zou, Y. Zhang, Noble metal-free hydrogen evolution catalysts for water splitting, Chem. Soc. Rev. 44 (2015) 5148-5180.

[74] P. Su, K. Iwase, S. Nakanishi, K. Hashimoto, K. Kamiya, Nickel-nitrogen-modified graphene: An efficient electrocatalyst for the reduction of carbon dioxide to carbon monoxide, Small 12 (2016) 6083-6089.

[75] D.L.T. Nguyen, Y. Kim, Y.J. Hwang, D.H. Won, Progress in development of electrocatalyst for CO_2 conversion to selective CO production, Carbon Energy 2 (2020) 72-98.

[76] J.T. Feaster, C. Shi, E.R. Cave, T. Hatsukade, D.N. Abram, K.P. Kuhl, C. Hahn, J.K. Nørskov, T.F. Jaramillo, Understanding selectivity for the electrochemical reduction of carbon dioxide to formic acid and carbon monoxide on metal electrodes, ACS Catal. 7 (2017) 4822-4827.

[77] J. Li, Y. Kuang, Y. Meng, X. Tian, W.H. Hung, X. Zhang, A. Li, M. Xu, W. Zhou, C.S. Ku, C.Y. Chiang, G. Zhu, J. Guo, X. Sun, H. Dai, Electroreduction of CO_2

to formate on a copper-based electrocatalyst at high pressures with high energy conversion efficiency, J. Am. Chem. Soc. 142 (2020) 7276-7282.

[78] J. Jin, J. Luo, L. Zan, T. Peng, One-pot synthesis of Cu-nanocluster-decorated brookite TiO_2 quasi-nanocubes for enhanced activity and selectivity of CO_2 photoreduction to CH_4, Chemphyschem 18 (2017) 3230-3239.

[79] V. Tripkovic, M. Vanin, M. Karamad, M.E. Björketun, K.W. Jacobsen, K.S. Thygesen, J. Rossmeisl, Electrochemical CO_2 and CO reduction on metal-functionalized porphyrin-like graphene, J. Phys. Chem. C 117 (2013) 9187-9195.

[80] W. Ju, A. Bagger, X. Wang, Y. Tsai, F. Luo, T. Möller, H. Wang, J. Rossmeisl, A.S. Varela, P. Strasser, Unraveling mechanistic reaction pathways of the electrochemical CO_2 reduction on Fe-N-C single-site catalysts, ACS Energy Lett. 4 (2019) 1663-1671.

[81] L. Chen, Z. Guo, X.G. Wei, C. Gallenkamp, J. Bonin, E. Anxolabehere-Mallart, K.C. Lau, T.C. Lau, M. Robert, Molecular catalysis of the electrochemical and photochemical reduction of CO_2 with earth-abundant metal complexes. selective production of CO vs HCOOH by switching of the metal center, J. Am. Chem. Soc. 137 (2015) 10918-10921.

[82] A.S. Varela, N. Ranjbar Sahraie, J. Steinberg, W. Ju, H.-S. Oh, P. Strasser, Metal-doped nitrogenated carbon as an efficient catalyst for direct CO_2 electroreduction to CO and hydrocarbons, Angew.Chem.Int.Ed. 54 (2015) 10758-10762.

[83] H. Zhong, F. Meng, Q. Zhang, K. Liu, X. Zhang, Highly efficient and selective CO_2 electro-reduction with atomic Fe-C-N hybrid coordination on porous carbon nematosphere, Nano Research 12 (2019) 2318-2323.

[84] C. Zhao, X. Dai, T. Yao, W. Chen, X. Wang, J. Wang, J. Yang, S. Wei, Y. Wu, Y. Li, Ionic exchange of metal-organic frameworks to access single nickel sites for efficient electroreduction of CO_2, J. Am. Chem. Soc. 139 (2017) 8078-8081.

[85] X.-M. Hu, H.H. Hval, E.T. Bjerglund, K.J. Dalgaard, M.R. Madsen, M.-M. Pohl, E. Welter, P. Lamagni, K.B. Buhl, M. Bremholm, M. Beller, S.U. Pedersen, T. Skrydstrup, K. Daasbjerg, Selective CO_2 reduction to CO in water using earth-abundant metal and nitrogen-doped carbon electrocatalysts, ACS Catal. 8 (2018) 6255-6264.

[86] A. Roy, D. Hursán, K. Artyushkova, P. Atanassov, C. Janáky, A. Serov, Nanostructured metal-N-C electrocatalysts for CO_2 reduction and hydrogen evolution reactions, Applied Catalysis B: Environmental 232 (2018) 512-520.

[87] F. Pan, W. Deng, C. Justiniano, Y. Li, Identification of champion transition metals centers in metal and nitrogen-codoped carbon catalysts for CO_2 reduction, Applied Catalysis B: Environmental 226 (2018) 463-472.

[88] L. Takele Menisa, P. Cheng, C. Long, X. Qiu, Y. Zheng, J. Han, Y. Zhang, Y. Gao, Z. Tang, Insight into atomically dispersed porous M-N-C single-site catalysts for electrochemical CO_2 reduction, Nanoscale 12 (2020) 16617-16626.

[89] C. Kim, Y.-K. Choe, D.H. Won, U. Lee, H.-S. Oh, D.K. Lee, C.H. Choi, S. Yoon, W. Kim, Y.J. Hwang, B.K. Min, Turning harmful deposition of metal impurities into activation of nitrogen-doped carbon catalyst toward durable electrochemical CO_2 reduction, ACS Energy Lett. 4 (2019) 2343-2350.

[90] Y. Chen, L. Zou, H. Liu, C. Chen, Q. Wang, M. Gu, B. Yang, Z. Zou, J. Fang, H. Yang, Fe and N Co-doped porous carbon nanospheres with high density of active sites for efficient CO_2 electroreduction, J. Phys. Chem. C 123 (2019) 16651-16659.

[91] T. Möller, W. Ju, A. Bagger, X. Wang, F. Luo, T. Ngo Thanh, A.S. Varela, J. Rossmeisl, P. Strasser, Efficient CO_2 to CO electrolysis on solid Ni–N–C catalysts at industrial current densities, Energy Environ. Sci. 12 (2019) 640-647.

[92] L. Delafontaine, T. Asset, P. Atanassov, Metal-nitrogen-carbon electrocatalysts for CO_2 reduction towards syngas generation, ChemSusChem 13 (2020) 1688-1698.

[93] Q. He, D. Liu, J.H. Lee, Y. Liu, Z. Xie, S. Hwang, S. Kattel, L. Song, J.G. Chen, Electrochemical conversion of CO_2 to syngas with controllable CO/H_2 ratios over Co and Ni single-atom catalysts, Angew. Chem. Int. Ed. 59 (2020) 3033-3037.

[94] Z. Zhao, X. Peng, X. Liu, X. Sun, J. Shi, L. Han, G. Li, J. Luo, Efficient and stable electroreduction of CO_2 to CH_4 on CuS nanosheet arrays, J. Mater. Chem. A 5 (2017) 20239-20243.

[95] L. Han, S. Song, M. Liu, S. Yao, Z. Liang, H. Cheng, Z. Ren, W. Liu, R. Lin, G. Qi, X. Liu, Q. Wu, J. Luo, H.L. Xin, Stable and efficient single-atom Zn catalyst for CO_2 reduction to CH_4, J. Am. Chem. Soc. 142 (2020) 12563-12567.

[96] E. González-Cervantes, A.A. Crisóstomo, A. Gutiérrez-Alejandre, A.S. Varela, Optimizing FeNC materials as electrocatalysts for the CO_2 reduction reaction: Heat-treatment temperature, structure and performance correlations, ChemCatChem 11 (2019) 4854-4861.

[97] T.N. Huan, N. Ranjbar, G. Rousse, M. Sougrati, A. Zitolo, V. Mougel, F. Jaouen, M. Fontecave, Electrochemical reduction of CO_2 catalyzed by Fe-N-C materials: A structure-selectivity study, ACS Catal. 7 (2017) 1520-1525.

[98] N. Leonard, W. Ju, I. Sinev, J. Steinberg, F. Luo, A.S. Varela, B. Roldan Cuenya, P. Strasser, The chemical identity, state and structure of catalytically active

centers during the electrochemical CO_2 reduction on porous Fe-nitrogen-carbon (Fe-N-C) materials, Chem. Sci. 9 (2018) 5064-5073.

[99] A. Serov, K. Artyushkova, P. Atanassov, Fe-N-C oxygen reduction fuel cell catalyst derived from carbendazim: Synthesis, structure, and reactivity, Adv. Energy Mater. 4 (2014) 1301375.

[100] I. Katsounaros, J.C. Meier, S.O. Klemm, A.A. Topalov, P.U. Biedermann, M. Auinger, K.J.J. Mayrhofer, The effective surface pH during reactions at the solid–liquid interface, Electrochem. Commun. 13 (2011) 634-637.

[101] X. Liu, P. Schlexer, J. Xiao, Y. Ji, L. Wang, R.B. Sandberg, M. Tang, K.S. Brown, H. Peng, S. Ringe, C. Hahn, T.F. Jaramillo, J.K. Norskov, K. Chan, pH effects on the electrochemical reduction of $CO_{(2)}$ towards C_2 products on stepped copper, Nat. Commun. 10 (2019) 32.

[102] A.S. Varela, M. Kroschel, N.D. Leonard, W. Ju, J. Steinberg, A. Bagger, J. Rossmeisl, P. Strasser, pH effects on the selectivity of the electrocatalytic CO_2 reduction on graphene-embedded Fe-N-C motifs: Bridging concepts between molecular homogeneous and solid-state heterogeneous catalysis, ACS Energy Lett. 3 (2018) 812-817.

[103] A.S. Varela, M. Kroschel, T. Reier, P. Strasser, Controlling the selectivity of CO_2 electroreduction on copper: The effect of the electrolyte concentration and the importance of the local pH, Catal. Today 260 (2016) 8-13.

[104] Y. Wu, Z. Jiang, X. Lu, Y. Liang, H. Wang, Domino electroreduction of CO_2 to methanol on a molecular catalyst, Nature 575 (2019) 639-642.

[105] Y. Wang, L. Cao, N.J. Libretto, X. Li, C. Li, Y. Wan, C. He, J. Lee, J. Gregg, H. Zong, D. Su, J.T. Miller, T. Mueller, C. Wang, Ensemble effect in bimetallic electrocatalysts for CO_2 reduction, J. Am. Chem. Soc. 141 (2019) 16635-16642.

[106] W. Wang, L. Shang, G. Chang, C. Yan, R. Shi, Y. Zhao, G.I.N. Waterhouse, D. Yang, T. Zhang, Intrinsic carbon-defect-driven electrocatalytic reduction of carbon dioxide, Adv. Mater. 31 (2019) 1808276.

[107] H. Wang, T. Maiyalagan, X. Wang, Review on recent progress in nitrogen-doped graphene: Synthesis, characterization, and its potential applications, ACS Catal. 2 (2012) 781-794.

[108] G.L. Chai, Z.X. Guo, Highly effective sites and selectivity of nitrogen-doped graphene/CNT catalysts for CO_2 electrochemical reduction, Chem. Sci. 7 (2016) 1268-1275.

[109] Y. Liu, J. Zhao, Q. Cai, Pyrrolic-nitrogen doped graphene: a metal-free electrocatalyst with high efficiency and selectivity for the reduction of carbon dioxide to formic acid: a computational study, Phys. Chem. Chem. Phys. 18 (2016) 5491-5498.

[110] J. Wang, X. Huang, S. Xi, J.M. Lee, C. Wang, Y. Du, X. Wang, Linkage effect in the heterogenization of cobalt complexes by doped graphene for electrocatalytic CO_2 reduction, Angew. Chem. Int. Ed. 58 (2019) 13532-13539.

[111] Z. Chen, K. Mou, S. Yao, L. Liu, Zinc-coordinated nitrogen-codoped graphene as an efficient catalyst for selective electrochemical reduction of CO_2 to CO, ChemSusChem 11 (2018) 2944-2952.

[112] A. Bagger, L. Arnarson, M.H. Hansen, E. Spohr, J. Rossmeisl, Electrochemical CO reduction: A property of the electrochemical interface, J. Am. Chem. Soc. 141 (2019) 1506-1514.

[113] N. Gupta, M. Gattrell, B. MacDougall, Calculation for the cathode surface concentrations in the electrochemical reduction of CO_2 in $KHCO_3$ solutions, J. Appl. Electrochem. 36 (2005) 161-172.

[114] Z. Qin, X. Wang, L. Dong, T. Su, B. Li, Y. Zhou, Y. Jiang, X. Luo, H. Ji, CO_2 methanation on Co/TiO_2 catalyst: Effects of Y on the support, Chem. Eng. Sci. 210 (2019) 115245.

[115] X. Sun, X. Kang, Q. Zhu, J. Ma, G. Yang, Z. Liu, B. Han, Very highly efficient reduction of CO_2 to CH_4 using metal-free N-doped carbon electrodes, Chem. Sci. 7 (2016) 2883-2887.

[116] J. Wu, M. Liu, P.P. Sharma, R.M. Yadav, L. Ma, Y. Yang, X. Zou, X.D. Zhou, R. Vajtai, B.I. Yakobson, J. Lou, P.M. Ajayan, Incorporation of nitrogen defects for efficient reduction of CO_2 via two-electron pathway on three-dimensional graphene foam, Nano Lett. 16 (2016) 466-470.

[117] Y. Huang, A.D. Handoko, P. Hirunsit, B.S. Yeo, Electrochemical reduction of CO_2 using copper single-crystal surfaces: Effects of CO* coverage on the selective formation of ethylene, ACS Catal. 7 (2017) 1749-1756.

[118] F. Li, M. Xue, G.P. Knowles, L. Chen, D.R. MacFarlane, J. Zhang, Porous nitrogen-doped carbon derived from biomass for electrocatalytic reduction of CO_2 to CO, Electrochim. Acta 245 (2017) 561-568.

[119] X. Li, W. Bi, M. Chen, Y. Sun, H. Ju, W. Yan, J. Zhu, X. Wu, W. Chu, C. Wu, Y. Xie, Exclusive Ni-N_4 sites realize near-unity CO selectivity for electrochemical CO_2 reduction, J. Am. Chem. Soc. 139 (2017) 14889-14892.

[120] Z. Zhao, X. Peng, X. Liu, X. Sun, J. Shi, L. Han, G. Li, J. Luo, Efficient and stable electroreduction of CO_2 to CH_4 on CuS nanosheet arrays, J. Mater. Chem. A 5 (2017) 20239-20243.

[121] W. Bi, X. Li, R. You, M. Chen, R. Yuan, W. Huang, X. Wu, W. Chu, C. Wu, Y. Xie, Surface immobilization of transition metal Ions on nitrogen-doped

graphene realizing high-efficient and selective CO_2 reduction, Adv. Mater. 30 (2018) 1706617.

[122] F. Pan, H. Zhao, W. Deng, X. Feng, Y. Li, A novel N,Fe-Decorated carbon nanotube/carbon nanosheet architecture for efficient CO_2 reduction, Electrochim. Acta 273 (2018) 154-161.

[123] Y. Pan, R. Lin, Y. Chen, S. Liu, W. Zhu, X. Cao, W. Chen, K. Wu, W.C. Cheong, Y. Wang, L. Zheng, J. Luo, Y. Lin, Y. Liu, C. Liu, J. Li, Q. Lu, X. Chen, D. Wang, Q. Peng, C. Chen, Y. Li, Design of single-atom Co-N_5 catalytic site: A robust electrocatalyst for CO_2 reduction with nearly 100% CO selectivity and remarkable stability, J. Am. Chem. Soc. 140 (2018) 4218-4221.

[124] F. Yang, P. Song, X. Liu, B. Mei, W. Xing, Z. Jiang, L. Gu, W. Xu, Highly efficient CO_2 electroreduction on ZnN_4-based single-atom catalyst, Angew. Chem. Int. Ed. 57 (2018) 12303-12307.

[125] H. Zhang, J. Wang, Z. Zhao, H. Zhao, M. Cheng, A. Li, C. Wang, J. Wang, J. Wang, The synthesis of atomic Fe embedded in bamboo-CNTs grown on graphene as a superior CO_2 electrocatalyst, Green Chemistry 20 (2018) 3521-3529.

[126] Y. Cheng, S. Zhao, H. Li, S. He, J.-P. Veder, B. Johannessen, J. Xiao, S. Lu, J. Pan, M.F. Chisholm, S.-Z. Yang, C. Liu, J.G. Chen, S.P. Jiang, Unsaturated edge-anchored Ni single atoms on porous microwave exfoliated graphene oxide for electrochemical CO_2, Applied Catalysis B: Environmental 243 (2019) 294-303.

[127] M. Kuang, A. Guan, Z. Gu, P. Han, L. Qian, G. Zheng, Enhanced N-doping in mesoporous carbon for efficient electrocatalytic CO_2 conversion, Nano Research 12 (2019) 2324-2329.

[128] D.C. Liu, T. Ouyang, R. Xiao, W.J. Liu, D.C. Zhong, Z. Xu, T.B. Lu, Anchoring Co^{II} ions into a thiol-laced metal-organic framework for efficient visible-light-driven conversion of CO_2 into CO, ChemSusChem 12 (2019) 2166-2170.

[129] C. Lu, J. Yang, S. Wei, S. Bi, Y. Xia, M. Chen, Y. Hou, M. Qiu, C. Yuan, Y. Su, F. Zhang, H. Liang, X. Zhuang, Atomic Ni anchored covalent triazine framework as high efficient electrocatalyst for carbon dioxide conversion, Adv. Funct. Mater. 29 (2019) 1806884.

[130] H. Ning, Q. Mao, W. Wang, Z. Yang, X. Wang, Q. Zhao, Y. Song, M. Wu, N-doped reduced graphene oxide supported Cu_2O nanocubes as high active catalyst for CO_2 electroreduction to C_2H_4, J. Alloys. Compd. 785 (2019) 7-12.

[131] W. Ren, X. Tan, W. Yang, C. Jia, S. Xu, K. Wang, S.C. Smith, C. Zhao, Isolated diatomic Ni-Fe metal-nitrogen sites for synergistic electroreduction of CO_2, Angew. Chem. Int. Ed. 58 (2019) 6972-6976.

[132] C.-Z. Yuan, H.-B. Li, Y.-F. Jiang, K. Liang, S.-J. Zhao, X.-X. Fang, L.-B. Ma, T. Zhao, C. Lin, A.-W. Xu, Tuning the activity of N-doped carbon for CO_2 reduction via in situ encapsulation of nickel nanoparticles into nano-hybrid carbon substrates, J. Mater. Chem. A 7 (2019) 6894-6900.

[133] B. Zhang, J. Zhang, J. Shi, D. Tan, L. Liu, F. Zhang, C. Lu, Z. Su, X. Tan, X. Cheng, B. Han, L. Zheng, J. Zhang, Manganese acting as a high-performance heterogeneous electrocatalyst in carbon dioxide reduction, Nat. Commun. 10 (2019) 2980.

[134] F. Pan, B. Li, E. Sarnello, Y. Fei, Y. Gang, X. Xiang, Z. Du, P. Zhang, G. Wang, H.T. Nguyen, T. Li, Y.H. Hu, H.C. Zhou, Y. Li, Atomically dispersed iron-nitrogen sites on hierarchically mesoporous carbon nanotube and graphene nanoribbon networks for CO_2 reduction, ACS Nano 14 (2020) 5506-5516.

[135] S. Wu, X. Lv, D. Ping, G. Zhang, S. Wang, H. Wang, X. Yang, D. Guo, S. Fang, Highly exposed atomic Fe-N active sites within carbon nanorods towards electrocatalytic reduction of CO_2 to CO, Electrochim. Acta 340 (2020) 135930.

[136] A. Hasani, M.A. Teklagne, H.H. Do, S.H. Hong, Q. Van Le, S.H. Ahn, S.Y. Kim, Graphene-based catalysts for electrochemical carbon dioxide reduction, Carbon Energy 2 (2020) 158-175.

[137] J.S. Yoo, R. Christensen, T. Vegge, J.K. Norskov, F. Studt, Theoretical insight into the trends that guide the electrochemical reduction of carbon dioxide to formic acid, ChemSusChem 9 (2016) 358-363.

[138] H.A. Hansen, J.B. Varley, A.A. Peterson, J.K. Norskov, Understanding trends in the electrocatalytic activity of metals and enzymes for CO_2 reduction to CO, J. Phys. Chem. Lett. 4 (2013) 388-392.

[139] Y. Hori, CO_2-reduction, catalyzed by metal electrodes, John Wiley & Sons, Ltd. (2010) https://doi.org/10.1002/9780470974001.f207055

[140] X. Nie, M.R. Esopi, M.J. Janik, A. Asthagiri, Selectivity of CO_2 reduction on copper electrodes: the role of the kinetics of elementary steps, Angew. Chem. Int. Ed. 52 (2013) 2459-2462.

[141] Y. Zheng, A. Vasileff, X. Zhou, Y. Jiao, M. Jaroniec, S.Z. Qiao, Understanding the roadmap for electrochemical reduction of CO_2 to multi-carbon oxygenates and hydrocarbons on copper-based catalysts, J. Am. Chem. Soc. 141 (2019) 7646-7659.

[142] A.A. Peterson, F. Abild-Pedersen, F. Studt, J. Rossmeisl, J.K. Nørskov, How copper catalyzes the electroreduction of carbon dioxide into hydrocarbon fuels, Energy Environ. Sci. 3 (2010) 1311-1315.

[143] K.J.P. Schouten, Y. Kwon, C.J.M. van der Ham, Z. Qin, M.T.M. Koper, A new mechanism for the selectivity to C_1 and C_2 species in the electrochemical reduction of carbon dioxide on copper electrodes, Chem. Sci. 2 (2011) 1902-1909.

[144] X. Wang, J.F. de Araujo, W. Ju, A. Bagger, H. Schmies, S. Kuhl, J. Rossmeisl, P. Strasser, Mechanistic reaction pathways of enhanced ethylene yields during electroreduction of CO_2-CO co-feeds on Cu and Cu-tandem electrocatalysts, Nat. Nanotechnol. 14 (2019) 1063-1070.

[145] L. Fan, C. Xia, F. Yang, J. Wang, H. Wang, Y. Lu, Strategies in catalysts and electrolyzer design for electrochemical CO_2 reduction toward C_{2+} products, Sci. Adv. 6 (2020) eaay3111.

[146] K.D. Yang, C.W. Lee, K. Jin, S.W. Im, K.T. Nam, Current status and bioinspired perspective of electrochemical conversion of CO_2 to a long-chain hydrocarbon, J. Phys. Chem. Lett. 8 (2017) 538-545.

[147] K.J. Schouten, Z. Qin, E. Perez Gallent, M.T. Koper, Two pathways for the formation of ethylene in CO reduction on single-crystal copper electrodes, J. Am. Chem. Soc. 134 (2012) 9864-9867.

[148] J.H. Montoya, C. Shi, K. Chan, J.K. Norskov, Theoretical Insights into a CO Dimerization Mechanism in CO_2 Electroreduction, J. Phys. Chem. Lett. 6 (2015) 2032-2037.

[149] D.H. Nam, P. De Luna, A. Rosas-Hernandez, A. Thevenon, F. Li, T. Agapie, J.C. Peters, O. Shekhah, M. Eddaoudi, E.H. Sargent, Molecular enhancement of heterogeneous CO_2 reduction, Nat. Mater. 19 (2020) 266-276.

[150] T. Asset, S.T. Garcia, S. Herrera, N. Andersen, Y. Chen, E.J. Peterson, I. Matanovic, K. Artyushkova, J. Lee, S.D. Minteer, S. Dai, X. Pan, K. Chavan, S.

Calabrese Barton, P. Atanassov, Investigating the nature of the active sites for the CO_2 reduction reaction on carbon-based electrocatalysts, ACS Catal. 9 (2019) 7668-7678.

[151] W. Ju, A. Bagger, G.P. Hao, A.S. Varela, I. Sinev, V. Bon, B. Roldan Cuenya, S. Kaskel, J. Rossmeisl, P. Strasser, Understanding activity and selectivity of metal-nitrogen-doped carbon catalysts for electrochemical reduction of CO_2, Nat. Commun. 8 (2017) 944.

[152] Z. Sun, T. Ma, H. Tao, Q. Fan, B. Han, Fundamentals and challenges of electrochemical CO_2 reduction using two-dimensional materials, Chem. 3 (2017) 560-587.

[153] F. Pan, H. Zhang, K. Liu, D. Cullen, K. More, M. Wang, Z. Feng, G. Wang, G. Wu, Y. Li, Unveiling active sites of CO_2 reduction on nitrogen-coordinated and atomically dispersed iron and cobalt catalysts, ACS Catal. 8 (2018) 3116-3122.

[154] Z.L. Wang, J. Choi, M. Xu, X. Hao, H. Zhang, Z. Jiang, M. Zuo, J. Kim, W. Zhou, X. Meng, Q. Yu, Z. Sun, S. Wei, J. Ye, G.G. Wallace, D.L. Officer, Y. Yamauchi, Optimizing electron densities of Ni-N-C complexes by hybrid coordination for efficient electrocatalytic CO_2 reduction, ChemSusChem 13 (2020) 929-937.

[155] J. Yang, D. Wang, Y. Li, Identifying the types and characterization of the active sites on M-X-C single-atom catalysts, Chemphyschem 21 (2020) 2486-2486.

[156] Y.N. Gong, L. Jiao, Y. Qian, C.Y. Pan, L. Zheng, X. Cai, B. Liu, S.H. Yu, H.L. Jiang, Regulating the coordination environment of MOF-templated single-atom nickel electrocatalysts for boosting CO_2 reduction, Angew. Chem. Int. Ed. 59 (2020) 2705-2709.

[157] S. Gao, Y. Lin, X. Jiao, Y. Sun, Q. Luo, W. Zhang, D. Li, J. yang, Y. Xie, Partially oxidized atomic cobalt layers for carbon dioxide electroreduction to liquid fuel, Nature 529 (2016) 68-71.

[158] L. Xu, F. Wang, M. Chen, J. Zhang, K. Yuan, L. Wang, K. Wu, G. Xu, W. Chen, CO_2 methanation over a Ni based ordered mesoporous catalyst for the production of synthetic natural gas, RSC Adv. 6 (2016) 28489-28499.

[159] D. Wu, X. Wang, X.-Z. Fu, J.-L. Luo, Ultrasmall Bi nanoparticles confined in carbon nanosheets as highly active and durable catalysts for CO_2 electroreduction, Applied Catalysis B: Environmental 284 (2021) 119723.

[160] W. Zhang, S. Yang, M. Jiang, Y. Hu, C. Hu, X. Zhang, Z. Jin, Nanocapillarity and nanoconfinement effects of pipet-like bismuth@carbon nanotubes for highly efficient electrocatalytic CO_2 reduction, Nano Lett. 21 (2021) 2650-2657.

[161] X. Wang, Y. Wang, X. Sang, W. Zheng, S. Zhang, L. Shuai, B. Yang, Z. Li, J. Chen, L. Lei, N.M. Adli, M.K.H. Leung, M. Qiu, G. Wu, Y. Hou, Dynamic activation of adsorbed intermediates via axial traction for the promoted electrochemical CO_2 reduction, Angew.Chem. Int. Ed. 60 (2021) 4192-4198.

[162] N. Sreekanth, M.A. Nazrulla, T.V. Vineesh, K. Sailaja, K.L. Phani, Metal-free boron-doped graphene for selective electroreduction of carbon dioxide to formic acid/formate, Chem. Commun. 51 (2015) 16061-16064.

[163] X. Wang, X. Sang, C.L. Dong, S. Yao, L. Shuai, J. Lu, B. Yang, Z. Li, L. Lei, M. Qiu, L. Dai, Y. Hou, Proton capture strategy for enhancing electrochemical CO_2 reduction on atomically dispersed metal-nitrogen active sites, Angew.Chem. Int. Ed. (2021) https://doi.org/10.1002/anie.202100011.

[164] Y. Li, J. Li, J. Huang, J. Chen, Y. Kong, B. Yang, Z. Li, L. Lei, G. Chai, Z. Wen, L. Dai, Y. Hou, Boosting electroreduction kinetics of nitrogen to ammonia via

tuning electron distribution of single-atomic iron sites, Angew.Chem. Int. Ed. 60 (2021) 9078-9085.

[165] W. Zheng, Y. Wang, L. Shuai, X. Wang, F. He, C. Lei, Z. Li, B. Yang, L. Lei, C. Yuan, M. Qiu, Y. Hou, X. Feng, Highly boosted reaction kinetics in carbon dioxide electroreduction by surface-introduced electronegative dopants, Adv. Funct. Mater. 31 (2021) 2008146.

[166] T. Wang, X. Sang, W. Zheng, B. Yang, S. Yao, C. Lei, Z. Li, Q. He, J. Lu, L. Lei, L. Dai, Y. Hou, Gas diffusion strategy for inserting atomic iron sites into graphitized carbon supports for unusually high-efficient CO_2 electroreduction and high-performance Zn-CO_2 batteries, Adv. Mater. 32 (2020) 2002430.

[167] X. Li, H. Rong, J. Zhang, D. Wang, Y. Li, Modulating the local coordination environment of single-atom catalysts for enhanced catalytic performance, Nano Research 13 (2020) 1842-1855.

[168] Y. Wang, Y. Liu, W. Liu, J. Wu, Q. Li, Q. Feng, Z. Chen, X. Xiong, D. Wang, Y. Lei, Regulating the coordination structure of metal single atoms for efficient electrocatalytic CO_2 reduction, Energy Environ. Sci. 13 (2020) 4609-4624.

[169] B. Lu, Q. Liu, S. Chen, Electrocatalysis of single-atom sites: Impacts of atomic coordination, ACS Catal. 10 (2020) 7584-7618.

[170] J. Zhang, Q.-a. Huang, J. Wang, J. Wang, J. Zhang, Y. Zhao, Supported dual-atom catalysts: Preparation, characterization, and potential applications, Chinese J. Catal. 41 (2020) 783-798.

[171] M. Zhao, Y. Huang, Y. Peng, Z. Huang, Q. Ma, H. Zhang, Two-dimensional metal-organic framework nanosheets: synthesis and applications, Chem. Soc. Rev. 47 (2018) 6267-6295.

[172] H. Li, L. Wang, Y. Dai, Z. Pu, Z. Lao, Y. Chen, M. Wang, X. Zheng, J. Zhu, W. Zhang, R. Si, C. Ma, J. Zeng, Synergetic interaction between neighbouring platinum monomers in CO_2 hydrogenation, Nat. Nanotechnol. 13 (2018) 411-417.

[173] M. Xiao, H. Zhang, Y. Chen, J. Zhu, L. Gao, Z. Jin, J. Ge, Z. Jiang, S. Chen, C. Liu, W. Xing, Identification of binuclear Co_2N_5 active sites for oxygen reduction reaction with more than one magnitude higher activity than single atom CoN_4 site, Nano Energy 46 (2018) 396-403.

[174] Y. Yan, K. Li, X. Chen, Y. Yang, J.M. Lee, Heterojunction-assisted Co_3S_4@Co_3O_4 core-shell octahedrons for supercapacitors and both oxygen and carbon dioxide reduction reactions, Small 13 (2017) 1701724.

[175] F. Li, X. Liu, Z. Chen, 1 + 1′ > 2: Heteronuclear biatom catalyst outperforms its homonuclear counterparts for CO oxidation, Small Methods 3 (2019) 1800480.

[176] G. Luo, Y. Jing, Y. Li, Rational design of dual-metal-site catalysts for electroreduction of carbon dioxide, J. Mater. Chem. A 8 (2020) 15809-15815.

[177] J. Resasco, L.D. Chen, E. Clark, C. Tsai, C. Hahn, T.F. Jaramillo, K. Chan, A.T. Bell, Promoter effects of alkali metal cations on the electrochemical reduction of carbon dioxide, J. Am. Chem. Soc. 139 (2017) 11277-11287.

[178] M.R. Singh, Y. Kwon, Y. Lum, J.W. Ager, 3rd, A.T. Bell, Hydrolysis of electrolyte cations enhances the electrochemical reduction of CO_2 over Ag and Cu, J. Am. Chem. Soc. 138 (2016) 13006-13012.

[179] P.J. Dyson, P.G. Jessop, Solvent effects in catalysis: rational improvements of catalysts via manipulation of solvent interactions, Catal. Sci. Technol. 6 (2016) 3302-3316.

[180] H. Wang, S. Xu, C. Tsai, Y. Li, C. Liu, J. Zhao, Y. Liu, H. Yuan, F. Abild-Pedersen, F.B. Prinz, J.K. Nørskov, Y. Cui, Direct and continuous strain control of catalysts with tunable battery electrode materials, Science 354 (2016) 1031-1036.

[181] A. Khorshidi, J. Violet, J. Hashemi, A.A. Peterson, How strain can break the scaling relations of catalysis, Nat. Catal. 1 (2018) 263-268.

[182] M. Luo, S. Guo, Strain-controlled electrocatalysis on multimetallic nanomaterials, Nat. Rev. Mater. 2 (2017) 17059.